Strong-field ionization of heteronuclear diatomic molecules using an orthogonally polarized two-color laser field

D. Habibović,[1] A. Gazibegović-Busuladžić,[1] M. Busuladžić,[2,1] and D. B. Milošević[1,3]
[1]*Faculty of Science, University of Sarajevo, Zmaja od Bosne 35, 71000 Sarajevo, Bosnia and Herzegovina*
[2]*Faculty of Medicine, University of Sarajevo, Čekaluša 90, 71000 Sarajevo, Bosnia and Herzegovina*
[3]*Academy of Sciences and Arts of Bosnia and Herzegovina, Bistrik 7, 71000 Sarajevo, Bosnia and Herzegovina*

(Received 18 January 2021; revised 19 March 2021; accepted 20 April 2021; published 4 May 2021)

We apply the improved molecular strong-field approximation to investigate high-order above-threshold ionization (HATI) of heteronuclear diatomic molecules by an orthogonally polarized two-color (OTC) laser field. The OTC field consists of two linearly polarized components with frequencies $r\omega$ and $s\omega$, where r and s are integers, and ω is the fundamental frequency. The molecule is aligned in the OTC laser field polarization plane. We show that the photoelectron momentum distribution obeys one reflection symmetry which is valid for arbitrary values of the relative phase between the OTC field components in the case when $r + s$ is odd. For molecules oriented along the polarization axis z_L of the $r\omega$ component ($\theta_L = 0^\circ$) and r even and s odd, the HATI spectrum exhibits the reflection symmetry with respect to the z_L axis. When the molecular orientation is along the x_L axis, which is perpendicular to the polarization axis of the $r\omega$ component ($\theta_L = 90^\circ$), the spectrum exhibits the reflection symmetry with respect to the x_L axis for r odd and s even. In addition, we analyze the asymmetry in the photoelectron spectra of heteronuclear molecules by comparing them with the photoelectron spectra obtained ionizing a homonuclear diatomic molecule. We also explore the influence of the shift of the relative phase by 180° on the HATI spectra. We explain some characteristics of the obtained HATI spectra using a generalization of the classical two-dimensional simple man's model which includes ionization probabilities calculated using the imaginary-time method. Finally, we analyze the interference minima for different heteronuclear diatomic molecules and for particular values of the emission angle, laser-field parameters, and internuclear distance. These minima are well fitted with the curve obtained using the derived condition for the two-center destructive interference minima.

DOI: 10.1103/PhysRevA.103.053101

I. INTRODUCTION

High-order nonlinear atomic and molecular processes are of great interest for understanding the laser-matter interactions (see review papers [1–11] and references therein). These processes have attracted a lot of attention over the past few decades because they occur on the subfemtosecond timescale, so that they can be used to study the electron dynamics in atoms and molecules. This opened up a new area of science, the so-called attoscience (see Refs. [3,5,7,8,10] and references therein). To observe high-order nonlinear processes strong laser fields are required. Sometimes, these processes are called laser-induced processes.

Among the laser-induced processes, high-order harmonic generation (HHG) and above-threshold ionization (ATI) are considered to be of particular importance. The usual way to describe the phenomenology of these processes is to use the so-called three-step model [12,13]. The first step accounts for ionization. In the second step, the liberated electron propagates under the influence of the laser field. If the laser field is strong enough, the interaction of the ionized electron with the parent ion can be neglected. This approximation is called the strong-field approximation (SFA). The third step is different for the HHG and ATI processes. If the ionized electron goes directly to the detector after the ionization, the process is denoted as the ATI process and these electrons are called the direct electrons. However, the laser field has an oscillatory character, and the ionized electron can be returned in the vicinity of the parent ion. In this case, two scenarios can happen. In the first one, the returned electron recombines with the parent ion, and the energy excess is emitted in the form of a high-energy photon. This corresponds to the HHG process. The second scenario corresponds to the situation when the returned electron elastically rescatters off the parent ion. Such an electron continues to accelerate in strong laser field, and contributes to the high-energy part of the photoelectron spectrum. This process is called high-order ATI (HATI) process and these photoelectrons are denoted as rescattered electrons (see recent review paper [14]). The high-energy part of the photoelectron spectrum exhibits a plateau-like structure, but the corresponding yield is much lower than that of the ATI process. The plateau is terminated by an abrupt cutoff. The HATI photoelectron momentum spectra can be used to extract accurate differential cross sections for electron elastic scattering off the target ion.

One approach to consider a quantum-mechanical problem is to solve the time-dependent Schrödinger equation. This approach is usually difficult and time-consuming even for simple

molecular systems [15–17] (see also Ref. [18] and references therein), so that it is practically applicable only for simplest homonuclear molecules like H_2 molecule, homonuclear H_2^+ ion, and heteronuclear HeH^{2+} ion. To avoid this difficulty, the physicists have developed various approximative methods, such as the mentioned SFA theory.

Let us now briefly comment on our theory of molecular strong-field ionization and its application to various laser-field configurations. In general, in the SFA the influence of the Coulomb potential is neglected in intermediate states. In Ref. [19], we developed our version of the molecular SFA (MSFA) which allows one to introduce the laser-field dressing of the initial bound state [20,21]. Next, we included an additional interaction of the ionized electron with the atomic centers. We named this theory the improved MSFA (IMSFA). It has first been applied to the case of a linearly polarized laser field [22,23], and later on generalized to the cases of different polarization such as elliptical [24] and circular [25], and bichromatic field configurations like bicircular [26–28], and, more recently, to orthogonally polarized two-color (OTC) laser field [29]. For a linearly polarized laser field and homonuclear diatomic molecule our theoretical results were confirmed in experiments [30–36]. In this paper, we analyze the HATI spectra of heteronuclear diatomic molecules. Our IMSFA theory for heteronuclear molecules and an elliptically polarized laser field was formulated in Refs. [37–39].

We analyze the HATI spectra obtained using an orthogonally polarized two-color laser field. The OTC field consists of two linearly polarized components with orthogonal polarizations and commensurable frequencies. In Ref. [29], we presented a list of references devoted to strong-field processes in OTC field. There is only a small number of papers in which the ionization of molecules by an OTC laser field was considered. We mention here Refs. [40–46], with the comment that the high-energy ATI spectra, which are caused by the rescattered electrons and are of main interest in our paper, are not considered in these references. Dissociative double ionization of CO in OTC laser fields was considered in Ref. [44]. The photoelectron circular dichroism in chiral molecules exposed to the OTC field was demonstrated in Ref. [45]. Using OTC laser fields it is possible to achieve a stronger molecular orientation [46]. In Ref. [29], we have included the rescattering effects for the homonuclear molecules in an OTC field. We analyzed the rotational and reflection symmetries of the HATI spectra. In addition, we observed the interference minima in the ionization yield as a function of the molecular orientation angle and the photoelectron energy. These minima are well-fitted with the curve obtained using the derived condition for the destructive interference minima.

As we have mentioned, the main goal of this paper is to study the HATI process on polar molecules which can possess a dipole moment due to the nonsymmetric distribution of the electron density around the two different atomic centers. Because of that, the laser-induced dipole and polarizability should be taken into account. Above-threshold ionization of heteronuclear and polar diatomic molecules have been investigated by different authors: Liao *et al.* [47] (phase dependence of HATI in asymmetric molecules), Znakovskaya *et al.* [48] (attosecond control of electron dynamics in CO; dissociative ionization of CO), Madsen *et al.* [49] (see also more recent paper [50] and references therein), Ren and Nakajima [51,52], Li *et al.* [53] (orientation dependence of the ionization of the CO and NO molecules in an intense femtosecond two-color laser field), Zhu *et al.* [54,55], Liu *et al.* [56] (fully differential measurement on ATI of CO molecule), Zhang *et al.* [57] (dynamic core polarization in strong-field ionization of CO molecules), Bian and Bandrauk [58] (orientation-dependent forward-backward photoelectron holography from asymmetric molecular ion HeH^{2+}), Endo *et al.* [59] (imaging electronic excitation of NO by ultrafast laser tunneling ionization), Wang *et al.* [60], Hoang *et al.* [61], Song *et al.* [62] (orientation-dependent strong-field dissociative single ionization of CO), Ito *et al.* [63] (rescattering photoelectron spectroscopy of heterodiatomic molecules NO and CO), Rottke *et al.* [64] (strong-field ionization of heteronuclear XeAr dimer), Wustelt *et al.* [65,66] (strong-field polarizability-enhanced dissociative ionization of HeH^+), He *et al.* [67], Endo *et al.* [68], Ding *et al.* [69–71], and Zhang *et al.* [72].

This paper is organized as follows. In Sec. II we briefly present the IMSFA for heteronuclear diatomic molecules in an OTC laser field. Rotational and reflection symmetries of the HATI spectra for various combinations of the frequencies of the OTC laser-field components are analyzed in Sec. III. We use these symmetries to explain some features of the HATI spectra. In Sec. IV, we present a two-dimensional simple man's model, supported by calculation of the ionization probabilities using the imaginary-time method. In Sec. V, we present the destructive interference condition for the CO and NO molecules and analyze it using the IMSFA and quantum-orbit theory. Finally, in Sec. VI, we summarize the paper and state our main conclusions. We use the atomic system of units ($\hbar = e = m_e = 4\pi\varepsilon_0 = 1$).

II. THEORY

The theory developed in Ref. [19] can be applied for an arbitrary diatomic molecule. We treat the diatomic molecule as a three-particle system: two atomic centers and one active electron. For heteronuclear molecules, the mass asymmetry parameter is

$$\lambda = (m_A - m_B)/(m_A + m_B), \tag{1}$$

where m_A and m_B are the masses of atomic centers A and B, respectively. The position of the electron relative to the atomic center is

$$\mathbf{r}_q = \mathbf{r} + \frac{q-\lambda}{2}\mathbf{R}, \tag{2}$$

where $\mathbf{r}$ is the electronic coordinate, $\mathbf{R}$ is the internuclear coordinate, and $q = 1$ ($q = -1$) corresponds to the atomic center A (B). The differential ionization rate for emission of an electron with the initial state i and the final momentum $\mathbf{k}_\mathrm{f}$ is

$$w_{\mathbf{R}\mathbf{k}_\mathrm{f}i} = 2\pi\,\mathbf{k}_\mathrm{f}\left|T_{\mathbf{R}\mathbf{k}_\mathrm{f}i}(n)\right|^2. \tag{3}$$

The T-matrix element $T_{\mathbf{R}\mathbf{k}_\mathrm{f}i}(n)$ can be written as

$$T_{\mathbf{R}\mathbf{k}_\mathrm{f}i}(n) = \int_0^T \frac{dt}{T}\left[\mathcal{F}^{(0)}_{\mathbf{R}\mathbf{k}_\mathrm{f}i}(t) + \mathcal{F}^{(1)}_{\mathbf{R}\mathbf{k}_\mathrm{f}i}(t)\right]e^{i[\mathcal{U}(t)+n\omega t]}, \tag{4}$$

where the superscript "(0)" ["(1)"] stands for the zeroth (first) order of expansion in the interaction of the atomic or ionic centers A and B with the electron in the absence of the laser field. Here

$$\mathcal{U}(t) = \mathbf{k}_\mathrm{f} \cdot \int^t dt' \mathbf{A}(t') + \int^t dt' \mathbf{A}^2(t')/2 - U_p t, \quad (5)$$

with U_p the ponderomotive energy, and $\mathbf{A}(t) = -\int^t dt'' \mathbf{E}(t'')$ the vector potential of the laser field. The zeroth-order T-matrix element, corresponding to direct electrons, consists of two contributions (we omit the subscript $\mathbf{R}\mathbf{k}_\mathrm{f} i$ for simplicity)

$$T^{(0)} = T^\mathrm{A} + T^\mathrm{B}, \quad (6)$$

where the contribution T^A (T^B) corresponds to the ionization from the center "A" ("B"). The first-order (rescattering) T-matrix element consists of four contributions [23]

$$T^{(1)} = T^\mathrm{AA} + T^\mathrm{BB} + T^\mathrm{AB} + T^\mathrm{BA}. \quad (7)$$

If the ionization and rescattering take place at the same center the corresponding T-matrix contributions are T^AA and T^BB. Also, the electron can be ionized at one center but rescattered off the other one. The corresponding T-matrix contributions are T^AB and T^BA. The partial contributions to the rescattering T-matrix element can interfere in a complicated manner, depending on molecular symmetry, orientation, and the electron emission angle.

Before we present the explicit form of the matrix elements $\mathcal{F}^{(0)}_{\mathbf{R}\mathbf{k}_\mathrm{f} i}(t)$ and $\mathcal{F}^{(1)}_{\mathbf{R}\mathbf{k}_\mathrm{f} i}(t)$, let us analyze the dressing of the initial bound state. To introduce this dressing we use the projection operator formalism of Refs. [20,73–75]. The main idea is to decompose the total state space into the subspace of bound states with the corresponding projection operator P_b, and the subspace of continuum states with the projection operator $P_c = 1 - P_b$. All results we obtained earlier for the atomic and molecular processes in a strong laser field remain valid if we replace the initial undressed ground state $|\psi_i(t)\rangle$ by the dressed ground state $|\widetilde{\psi}_i(t)\rangle$ restricted to the subspace of bound states [20,75]. Under the influence of the laser field the state $|\psi_i(t')\rangle$ evolves to the state $|\widetilde{\psi}_i(t)\rangle$ according to

$$|\widetilde{\psi}_i(t)\rangle = \lim_{t' \to -\infty} U_{bb}(t, t')|\psi_i(t')\rangle. \quad (8)$$

The evolution operator $U_{bb}(t, t') = P_b U(t, t') P_b$ is exact, but restricted to the subspace of bound states. The dressed bound state can be found using the second-order perturbation theory and assuming the low laser-field frequency [76]. This state has the following form:

$$|\widetilde{\psi}_i(t)\rangle = e^{i\boldsymbol{\mu}\cdot\int^t \mathbf{E}(t')dt' + \frac{i}{2}\sum_{jk}\alpha_{jk}\int^t E_j(t')E_k(t')dt'}|\psi_i(t)\rangle, \quad (9)$$

where $\boldsymbol{\mu}$ is the molecular dipole, and α_{jk} are the components of the polarizability tensor [77]. This approximation leads to the replacement of the ionization potential I_p from the undressed state $|\psi_i(t)\rangle = |\psi_i\rangle \exp(i\int^t I_p dt')$, by

$$I_p^d(t) = I_p + \boldsymbol{\mu}\cdot\mathbf{E}(t) + \frac{1}{2}\sum_{jk}\alpha_{jk}E_j(t)E_k(t). \quad (10)$$

The quantities $\boldsymbol{\mu}$ and α_{jk} can be calculated using the quantum chemistry softwares [78,79]. The time-independent part of the molecular orbital $|\psi_i(t)\rangle$ is written as a linear combination of the atomic orbitals $|\psi_a\rangle$, i.e., as $\sum_q \sum_a c_{qa}|\psi_a(\mathbf{r}_q)\rangle$ [37].

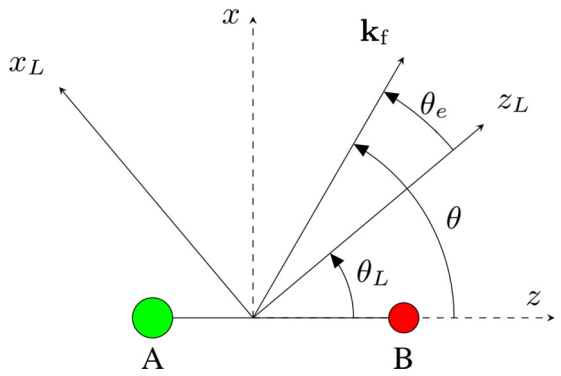

FIG. 1. The coordinate systems used in the paper. The diatomic molecule is placed along the z axis. The angle θ_L describes the position of the molecule AB relative to the laser field. The photoelectron emission angle is θ_e (θ) relative to the z_L (z) axis.

The geometry and the coordinate systems used in our paper are defined in Fig. 1. The molecular and laser-field coordinate systems are defined by the unit vectors $\hat{\mathbf{e}}_z$ and $\hat{\mathbf{e}}_x$ and $\hat{\mathbf{e}}_{z_L}$ and $\hat{\mathbf{e}}_{x_L}$, respectively. These systems are coplanar and the diatomic molecule is placed along the z axis of the molecular coordinate frame. The position of the molecule relative to the laser field is described by the angle θ_L. The angles θ_e and θ are the photoelectron emission angles relative to the z_L and z axes, respectively. In the so defined coordinate system our OTC laser field is

$$\mathbf{E}(t) = E_1 \sin(r\omega t)\hat{\mathbf{e}}_{z_L} + E_2 \sin(s\omega t + \varphi)\hat{\mathbf{e}}_{x_L}, \quad (11)$$

where E_j is the electric field amplitude ($j = 1, 2$), $r\omega$ and $s\omega$ are integer multiples of the fundamental angular frequency ω, and φ is the relative phase between the two laser-field components. The laser-field components parallel and perpendicular to the molecular axis are

$$\begin{aligned} E_\parallel &= E_1 \sin(r\omega t)\cos\theta_L - E_2 \sin(s\omega t + \varphi)\sin\theta_L, \\ E_\perp &= E_1 \sin(r\omega t)\sin\theta_L + E_2 \sin(s\omega t + \varphi)\cos\theta_L. \end{aligned} \quad (12)$$

For diatomic molecules, only the diagonal elements of the polarizability tensor are different from zero, so that the third term on the right-hand side in (10) is $[\alpha_\parallel E_\parallel(t)^2 + \alpha_\perp E_\perp(t)^2]/2$. Here, $\alpha_\parallel$ ($\alpha_\perp$) is the polarizability parallel (perpendicular) to the internuclear axis. The molecular dipole is along the z axis, i.e., $\boldsymbol{\mu} = -\mu\hat{\mathbf{e}}_z$. For the OTC laser field (11), we have

$$\begin{aligned} \mu_S(t) &= \int^t \boldsymbol{\mu}\cdot\mathbf{E}(t')dt' \\ &= \mu[A_1 \cos(r\omega t)\cos\theta_L - A_2 \cos(s\omega t + \varphi)\sin\theta_L], \\ \alpha_S(t) &= \frac{1}{2}\int^t [\alpha_\parallel E_\parallel^2(t') + \alpha_\perp E_\perp^2(t')]dt' + \Delta_S, \end{aligned} \quad (13)$$

where $A_1 = E_1/(r\omega)$ and $A_2 = E_2/(s\omega)$. The time-independent part of the polarizability term leads to the Stark shift

$$\begin{aligned} \Delta_S = -\tfrac{1}{4}\big[&\alpha_\parallel\big(E_1^2\cos^2\theta_L + E_2^2\sin^2\theta_L\big) \\ &+ \alpha_\perp\big(E_1^2\sin^2\theta_L + E_2^2\cos^2\theta_L\big)\big]. \end{aligned} \quad (14)$$

The matrix element $\mathcal{F}^{(0)}_{\mathbf{R}\mathbf{k}_f i}(t)$, given by

$$\mathcal{F}^{(0)}_{\mathbf{R}\mathbf{k}_f i}(t) = e^{i[\mu_S(t)+\alpha_S(t)]} \sum_{q=\pm 1} e^{i(q-\lambda)[\mathbf{k}_f+\mathbf{A}(t)]\cdot\mathbf{R}/2} \times \sum_a c_{qa}\langle \mathbf{k}_f + \mathbf{A}(t)|\mathbf{E}(t)\cdot\mathbf{r}|\psi_a\rangle, \quad (15)$$

describes the direct electrons, which are ionized at the center $q = \pm 1$, while the rescattered electrons are described by

$$\mathcal{F}^{(1)}_{\mathbf{R}\mathbf{k}_f i}(t) = -ie^{-iS_{\mathbf{k}_{st}}(t)} \int_0^\infty d\tau \left(\frac{2\pi}{i\tau}\right)^{3/2} e^{i(\Delta_S - I_p)\tau} \times \sum_{q,q'} e^{i\{(q-\lambda)[\mathbf{k}_{st}+\mathbf{A}(t_0)]-(q'-\lambda)\mathbf{K}\}\cdot\mathbf{R}/2} \times V^{q'}_{e\mathbf{K}} e^{i[S_{\mathbf{k}_{st}}(t_0)+\mu_S(t_0)+\alpha_S(t_0)]} \times \sum_a c_{qa}\langle \mathbf{k}_{st} + \mathbf{A}(t_0)|\mathbf{E}(t_0)\cdot\mathbf{r}|\psi_a\rangle, \quad (16)$$

where $t_0 = t - \tau$, $\mathbf{K} = \mathbf{k}_{st} - \mathbf{k}_f$, $\mathbf{k}_{st} = -\int_{t_0}^t dt''\mathbf{A}(t'')/\tau$ is the stationary electron momentum, $S_{\mathbf{k}}(t) = \int^t dt''[\mathbf{k} + \mathbf{A}(t'')]^2/2$, and $V^{q'}_{e\mathbf{K}}$ is the Fourier transform of the rescattering potential at the corresponding atomic center $q' = \pm 1$. The energy-conservation condition is $n\omega = E_{\mathbf{k}_f} + U_p + I_p - \Delta_S$, where $E_{\mathbf{k}_f} = \mathbf{k}_f^2/2$ and $n = n_1 r + n_2 s$, with n_1 (n_2) the number of absorbed photons of frequency $r\omega$ ($s\omega$).

As examples of heteronuclear diatomic molecules we consider the CO and NO molecules. The equilibrium internuclear distance of CO is $R = 2.132$ a.u. and its ionization energy is $I_p = 14.014$ eV, while for NO we have $R = 2.1747$ a.u. and $I_p = 9.264$ eV. A detailed description of the method we used to obtain the values of the dipole moment and the two components of the polarizability tensor can be found in Ref. [37]. For the CO molecule, these values are $\mu = 1.055$ a.u., $\alpha_\parallel = 5.3673$ a.u., and $\alpha_\perp = 5.49$ a.u. A similar approach can be applied to the case of the NO molecule. For this molecule, the polarizability can be neglected, while the dipole moment is $\mu = 0.28$ a.u. Also, for comparison we use the N_2 molecule as an example of the homonuclear diatomic molecules. The equilibrium internuclear distance and the ionization energy of the N_2 molecule are $R = 2.282$ a.u. and $I_p = 12.3$ eV, respectively.

III. SYMMETRY CONSIDERATIONS

In this paper we assume that the amplitudes of the OTC electric field (11) are equal ($E_1 = E_2 = E_L$). However, the equality of the electric-field amplitudes is not the condition for the presented symmetries. The final momentum $\mathbf{k}_f$ is defined in the $z_L x_L$ coordinate system. For an arbitrary relative phase φ the time transformation $t \to t + T/2$ leads to the following electric-field transformation: $E_{z_L}(t + T/2) = (-1)^r E_{z_L}(t)$, $E_{x_L}(t + T/2) = (-1)^s E_{x_L}(t)$. The same transformation is valid for the vector $\mathbf{A}(t)$ [29]. If both r and s are odd, the time transformation $t \to t + T/2$ leads to the rotation by 180° about the y axis, i.e.,

$$\mathbf{E}(t + T/2) = R_y(\pi)\mathbf{E}(t) = -\mathbf{E}(t), \quad r + s \text{ even}, \quad (17)$$

where the rotation is described by the rotation matrix $R_y(\pi)$. If $r + s$ is odd, the time translation $t \to t + T/2$ changes the sign of the field component that oscillates with the odd multiple of the fundamental frequency, while the other one remains unchanged. This corresponds to the reflection with respect to the axis along which the field component, having frequency equal to the even multiple of the fundamental frequency, oscillates. The time-shift transformation $t \to t + T/2$ leads to

$$\mathbf{E}(t + T/2) = P_{z_L}\mathbf{E}(t), \quad r \text{ odd}, \quad s \text{ even}, \quad (18)$$

$$\mathbf{E}(t + T/2) = P_{x_L}\mathbf{E}(t), \quad r \text{ even}, \quad s \text{ odd}, \quad (19)$$

where we have introduced the parity operators P_{z_L} and P_{x_L}.

Heteronuclear diatomic molecules have only trivial C_1 rotational symmetry so that we cannot use the rotational symmetry (17) of the OTC field to reveal the symmetry of the photoelectron spectra, as we have done for homonuclear diatomic molecules. However, for particular molecular orientations we can use the reflection symmetries (18) and (19) for this purpose. In particular, for $\theta_L = 0°$ the molecule is invariant with respect to the reflection P_{x_L} so that we can use the dynamical symmetry (19) of the OTC field having r even and s odd. Analogously, for $\theta_L = \pm 90°$ heteronuclear diatomic molecules are invariant with respect to the reflection P_{z_L} and we can use the relation (18). The above symmetry follows from the trivial property of a diatomic molecule that it is invariant under the reflection with respect to its own internuclear axis. General reflection symmetries are considered in Appendix. The above symmetries are illustrated in Fig. 5, where the lower left panel corresponds to the case where r is odd, s is even, $\theta_L = 90°$, and the reflection symmetry is P_{z_L}, while the upper right panel corresponds to r even, s odd, $\theta_L = 0°$, and the symmetry is P_{x_L}.

A. Rotational symmetry

The heteronuclear diatomic molecules, unlike the homonuclear ones, have only a trivial rotational symmetry (C_1) as we stated earlier. As a consequence, the laser-molecule system also possesses only the C_1 rotational symmetry. Let us first consider the case of $r + s$ even. The time transformation $t \to t + T/2$ leads to the rotation of the field according to Eq. (17). However, the heteronuclear molecule is not invariant with respect to the rotation by 180° with respect to the y axis. Therefore the corresponding HATI spectra do not exhibit rotational symmetry unlike the case of homonuclear diatomic molecules. This is illustrated in Fig. 2 where the HATI photoelectron spectra of the CO molecule are presented in the momentum plane, with $k_z = \mathbf{k}_f \cdot \hat{\mathbf{e}}_{z_L}$ and $k_x = \mathbf{k}_f \cdot \hat{\mathbf{e}}_{x_L}$, for the ω-3ω OTC field having the relative phase $\varphi = 0°$, and for the molecular orientation angles $\theta_L = 30°$ (left panel) and $\theta_L = 30° + 180° = 210°$ (right panel). The HATI spectra in Fig. 2 themselves obey only the C_1 symmetry. However, rotation of the molecule by 180° with respect to the y axis leads to the rotation of the HATI photoelectron spectrum correspondingly. Rotating the left panel of Fig. 2 by 180° about the axis perpendicular to the polarization plane it becomes identical to the right panel.

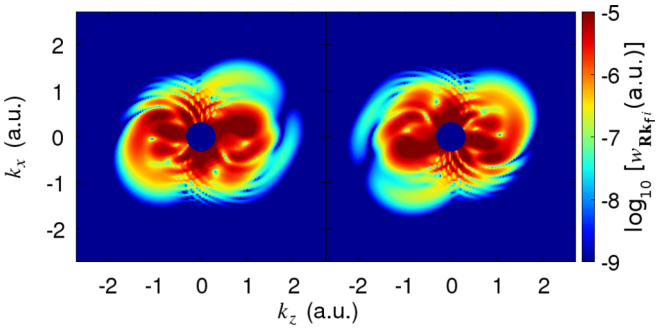

FIG. 2. Logarithm of the differential ionization rate of the CO molecule presented in false colors in the photoelectron momentum plane for the case of ionization by the ω-3ω OTC laser field having the relative phase $\varphi = 0^\circ$. Molecular orientation angles are $\theta_L = 30^\circ$ (left) and 210° (right). The results are obtained using the IMSFA. The intensity of the laser-field components is $E_L^2 = 0.9 \times 10^{14}$ W/cm^2. The fundamental wavelength is chosen so that $r\omega$ corresponds to 800 nm.

B. Reflection symmetries

We now consider the case where $r + s$ is odd. The time transformation $t \to t + T/2$ leads to the reflection of the field according to (18) for r odd and (19) for s odd.

First, we analyze the case where r is odd, while s is even. Using the symmetry transformation (18), and analogous relation for $\mathbf{A}(t)$, we obtain that the differential ionization rate $w_{\mathbf{Rk}_f i}(n)$ is invariant under the transformation

$$\theta \to -\theta, \quad \theta_L \to 180^\circ - \theta_L,$$
$$\theta_e \to 180^\circ - \theta_e, \quad r \text{ odd}, \ s \text{ even}. \tag{20}$$

This is illustrated in Fig. 3 where the HATI spectra obtained exposing the CO molecule to the ω-2ω OTC laser field for $\theta_L = 45^\circ$ (left panel) and $\theta_L = 135^\circ$ (right panel) are presented. The spectrum calculated for $\theta_L = 45^\circ$ is the mirror image of the spectrum calculated for $\theta_L = 135^\circ$, in accordance with the transformation (20).

In the second case where r is even, while s is odd, the differential ionization rate is invariant under the transformation

$$\theta \to -\theta, \quad \theta_L \to -\theta_L, \quad \theta_e \to -\theta_e, \quad r \text{ even}, \ s \text{ odd}. \tag{21}$$

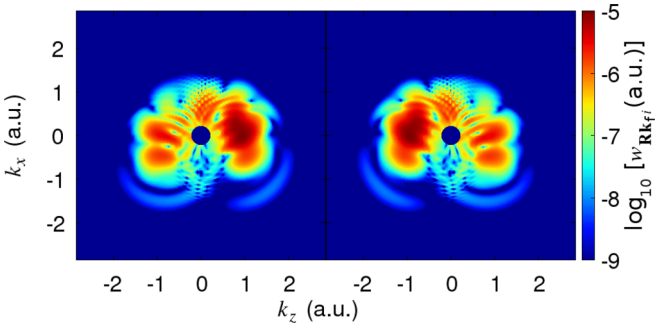

FIG. 3. Logarithm of the differential ionization rate of the CO molecule presented in false colors in the photoelectron momentum plane for the case of ionization by the ω-2ω OTC laser field having the relative phase $\varphi = 45^\circ$. Molecular orientation angles are $\theta_L = 45^\circ$ (left) and 135° (right). The results are obtained using the IMSFA. Other parameters are the same as in Fig. 2.

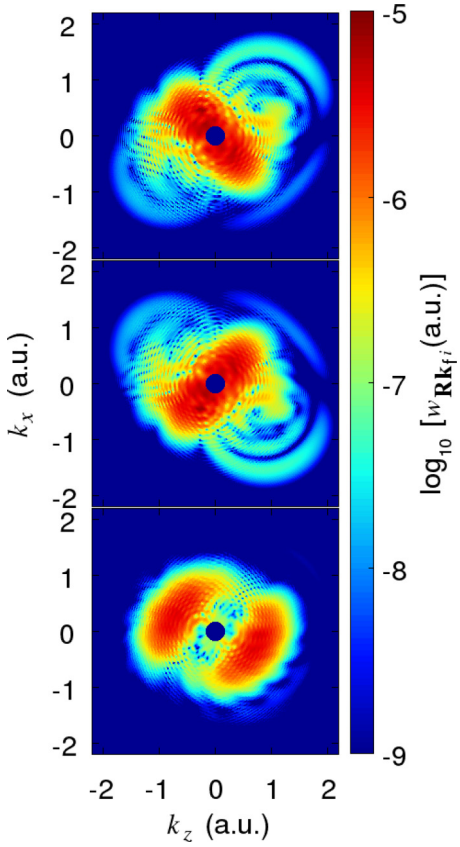

FIG. 4. Logarithm of the differential ionization rate of the CO molecule presented in false colors in the photoelectron momentum plane for the case of ionization by the 2ω-3ω OTC laser field having the relative phase $\varphi = 45^\circ$. Molecular orientation angles are $\theta_L = 45^\circ$ (top), -45° (middle), and 135° (bottom). The results are obtained using the IMSFA. Other parameters are the same as in Fig. 2.

This is illustrated in Fig. 4 where the HATI spectra of the CO molecule obtained by the 2ω-3ω OTC laser field for $\theta_L = 45^\circ$ (top panel) and $\theta_L = -45^\circ$ (middle panel) are presented. The spectrum calculated for $\theta_L = 45^\circ$ is the mirror image of the spectrum calculated for $\theta_L = -45^\circ$, in accordance with the transformation (21). However, the heteronuclear molecule is not invariant under the rotation by 180°, so that the spectra obtained for $\theta_L = -45^\circ$ are not the same as the spectra obtained for $\theta_L = 135^\circ$. The latter one is presented in the bottom panel of Fig. 4.

Let us now consider special cases where the molecular orientation is $\theta_L = 0^\circ$ or $\theta_L = 90^\circ$. Reflection of the coordinate system with respect to the z_L axis (P_{x_L}) leaves the molecular orientation $\theta_L = 0^\circ$ of a heteronuclear diatomic molecule (or linear molecule generally) virtually unchanged. This is not valid in the case of the reflection of the coordinate system with respect to x_L axis (P_{z_L}) unless the molecule is homonuclear (or symmetric linear molecule). Also, the molecular orientation $\theta_L = 90^\circ$ is virtually unchanged by the reflection P_{z_L}, but for the reflection P_{x_L} this is not true unless the molecule is

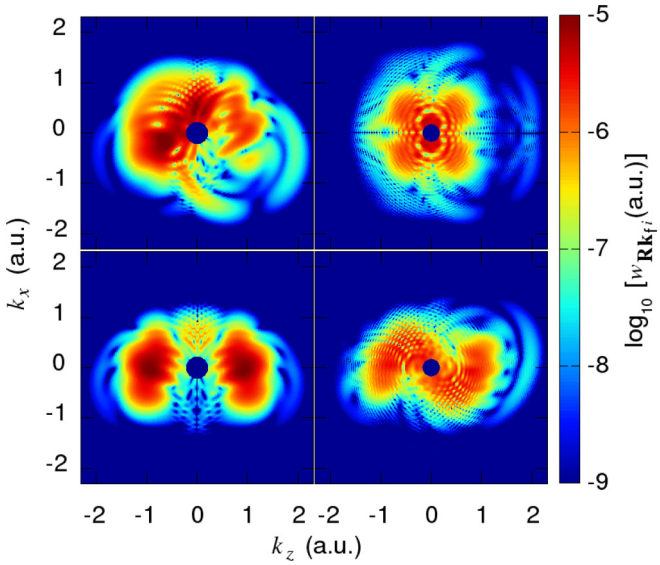

FIG. 5. Logarithm of the differential ionization rate of the CO molecule presented in false colors in the photoelectron momentum plane for the case of ionization by the ω-2ω (left) and 2ω-3ω (right) OTC laser field having the relative phase $\varphi = 45^\circ$. Molecular orientation angle is $\theta_L = 0^\circ$ for the upper panels and $\theta_L = 90^\circ$ for the lower panels. The results are obtained using the IMSFA. Other parameters are the same as in Fig. 2.

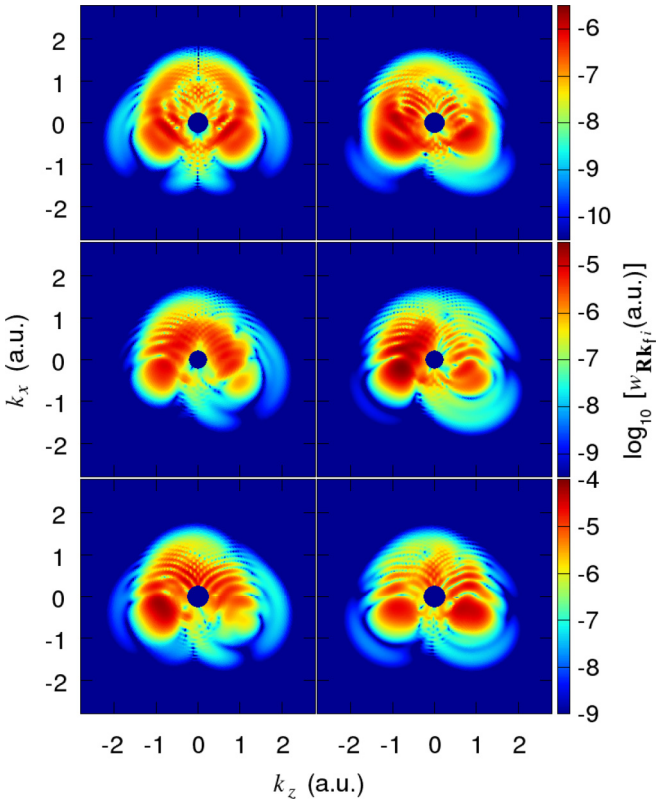

FIG. 6. Logarithm of the differential ionization rate of the N_2 (top), CO (middle), and NO (bottom) molecules presented in false colors in the photoelectron momentum plane for the case of ionization by the ω-2ω OTC laser field having the relative phase $\varphi = 0^\circ$. Molecular orientation angles are $\theta_L = 0^\circ$ (left) and -45° (right). The results are obtained using the IMSFA. Other parameters are the same as in Fig. 2.

homonuclear or linear symmetric. These symmetries lead to the specific symmetries of the HATI spectra if the laser field obeys similar symmetries. This is illustrated in Fig. 5 using the CO molecule irradiated by the ω-2ω (left column) and 2ω-3ω (right column) OTC laser fields. We see that for the molecular orientation $\theta_L = 0^\circ$ the spectrum obtained using 2ω-3ω OTC laser field possesses the reflection symmetry with respect to the k_z axis, i.e., it is invariant under the reflection P_{x_L} (see the upper right panel in Fig. 5). This is the case because the relation (21) is valid, and this reflection leaves the molecular orientation virtually unchanged. However, for the ω-2ω OTC laser field, the valid symmetry transformation of the field is (20), so that the HATI spectrum for $\theta_L = 0^\circ$ does not obey the reflection symmetry (see the upper left panel in Fig. 5). The situation is opposite if the molecular orientation angle is $\theta_L = 90^\circ$. In this case, the molecule is virtually unchanged by the reflection P_{z_L}, so that the HATI spectrum obtained using the ω-2ω OTC laser field possesses reflection symmetry with respect to the k_x axis (see the lower left panel in Fig. 5), while the reflection symmetry is absent for the 2ω-3ω OTC laser field (see the lower right panel in Fig. 5). It is also obvious that this molecular orientation is the only orientation in the laser polarization plane for which the photoelectron momentum spectrum, obtained using an $r\omega$−$s\omega$ OTC laser field, r odd and s even, is symmetric with respect to the x_L axis.

We conclude this subsection with a few words about the asymmetry in the photoelectron momentum distribution. For homonuclear diatomic molecules the electron probability density for the highest-occupied molecular orbital is symmetric with respect to the reflection about the molecular axis, and the axis perpendicular to the molecular axis. In the case of heteronuclear diatomic molecules, the reflection symmetry about the axis perpendicular to the molecular axis is absent. Using the saddle-point approximation it was explained in Ref. [41] that the photoelectron momentum distribution for homonuclear diatomic molecules is asymmetric in the ω-2ω field, even if the field obeys the symmetry relation (20), if the orientation of the molecule is different than $\theta_L = 0^\circ$ or $\theta_L = 90^\circ$. In Ref. [41], the contributions of the rescattered photoelectrons are not taken into account. To analyze the asymmetry properties of the photoelectron momentum distribution, we also take the ω-2ω OTC laser field as an example. In Fig. 6, we present the differential ionization rate of the N_2 (top panels), CO (middle panels), and NO (bottom panels) molecules. Molecular orientation angles are $\theta_L = 0^\circ$ (left panels) and $\theta_L = -45^\circ$ (right panels). For the N_2 molecule with the orientation $\theta_L = 0^\circ$, the spectra possess the reflection symmetry with respect to the k_x axis. However, for the orientation $\theta_L = -45^\circ$ the asymmetry in the photoelectron momentum distribution is clearly visible. This asymmetry in the field that obeys the transformation rule (18) (that corresponds to the ω-2ω OTC laser field) is a consequence of the molecular orientation. For heteronuclear molecules in this field, the photoelectron distribution manifests asymmetry for all planar molecular orientations except for $\theta_L = 90^\circ$. To illustrate this asymmetry

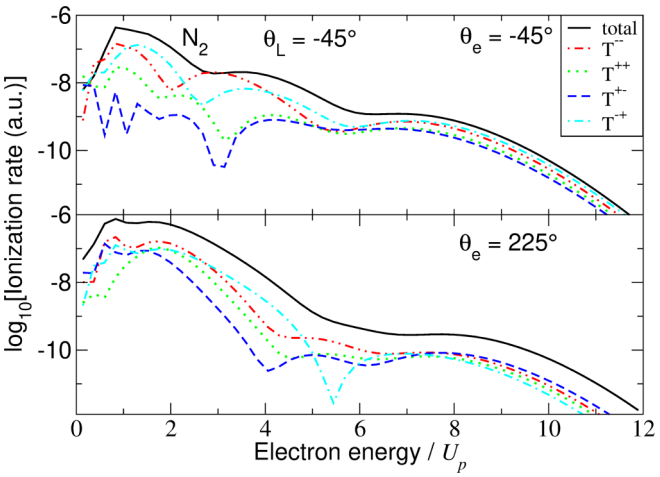

FIG. 7. Logarithm of the differential ionization rate of the N_2 molecule as a function of the electron kinetic energy $E_{\mathbf{k}_f}$ in units of the ponderomotive energy, for the case of ionization by the ω-2ω OTC laser field having the relative phase $\varphi = 0^\circ$. Molecular orientation angle is $\theta_L = -45^\circ$, and the electron emission angle is $\theta_e = -45^\circ$ ($\theta_e = 225^\circ$) for the upper (lower) panel. The total HATI rate includes all partial contributions to the rescattering T-matrix element. Various partial contributions are also presented. The results are obtained using the IMSFA. Other parameters are the same as in Fig. 2.

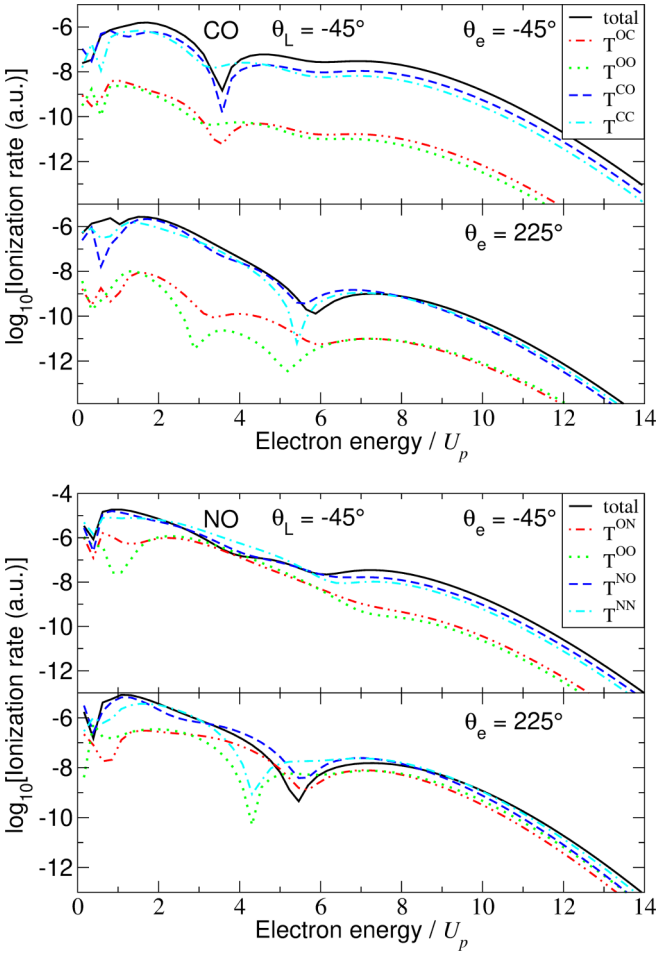

FIG. 8. Same as in Fig. 7, but for the CO molecule (top) and NO molecule (bottom).

we present the photoelectron momentum spectra of the CO molecule (middle panels) and NO molecule (bottom panels) for the case of the ionization by the ω-2ω OTC laser field. The asymmetry is clearly visible for both orientations. This asymmetry in the photoelectron spectra of the CO and NO molecules is, in general, a consequence of both the molecular asymmetry and the molecular orientation. For molecular orientation $\theta_L = 0^\circ$ the asymmetry in the photoelectron spectra of heteronuclear molecules is present due to the fact that a heteronuclear molecule does not obey the reflection symmetry with respect to the axis perpendicular to the internuclear axis.

In order to better understand the asymmetries observed in Fig. 6, we now analyze the partial-differential-ionization-rate contributions to the photoelectron spectra. First, in Fig. 7, we present the total HATI spectra of the N_2 molecule and all partial contributions as a function of the electron kinetic energy $E_{\mathbf{k}_f}$ for the relative phase $\varphi = 0^\circ$ and the molecular orientation $\theta_L = -45^\circ$. The partial contributions are denoted by T^{++}, T^{--}, T^{+-}, and T^{-+}. The contributions T^{++} and T^{--} correspond to the cases where the electron is ionized and rescattered at the same atomic center. In the case of contributions T^{+-} and T^{-+} ionization and rescattering take place at different atomic centers. From Fig. 7, we see that for the emission angle $\theta_e = 225^\circ$ the partial contributions clearly interfere constructively. On the other hand, for $\theta_e = -45^\circ$ though the total interference is constructive, the rates for the partial contributions and the total rate are within one order of magnitude. These results are explained by the fact that, for different values of θ_e and different ionization and rescattering centers, the photoelectron paths are different. This difference in paths, which also depends on the molecular orientation angle θ_L, is the cause of different interference behavior and the asymmetries which can be seen in the top right panel of Fig. 6.

In Fig. 8, we present the total and partial differential ionization rates for CO and NO molecules in the same way as in Fig. 7. The most prominent feature in the upper panels is that the contributions corresponding to the ionization from the carbon atom are dominant. This is the consequence of the electron-ground-state probability density distribution. This allows one to approximate the photoelectron spectra using only the contributions to the T-matrix element corresponding to the ionization from the carbon atom. Also, it is clear that the plateau structures are more developed for the emission angle $\theta_e = -45^\circ$. The partial contributions T^{CO} and T^{CC} interfere constructively (except near the energy $3.5U_p$) so that the total differential ionization rate is almost four times higher than the rate calculated using only one of these partial contributions. The situation is different for the emission angle $\theta_e = 225^\circ$. Here the total ionization rate is practically equal to the rate calculated using only partial contributions. Similar calculations are done for the NO molecule (see the lower panels in Fig. 8). In this case, the electron-ground-state probability density distribution is more homogeneous and, in general, all partial contributions to the T-matrix element are significant.

We see that the contributions of the electron that was ionized at the oxygen atom cannot be neglected and it varies with the molecular orientation in general. Here the constructive interference is present in the high-energy part of the spectrum for the emission angle $\theta_e = -45^\circ$, while for the emission angle $\theta_e = 225^\circ$ the total differential ionization rate is practically equal to the rates calculated using only partial contributions. In general, for the emission angles θ_e and $180^\circ - \theta_e$ the interference of partial contributions is different. This complicated interference leads to the asymmetry in the spectrum of the emitted electrons, as can be seen in the right panels of Fig. 6.

C. Shift of the relative phase by 180°

Let us now analyze what happens with the HATI spectra if the relative phase φ is changed to $\varphi + 180^\circ$. This phase shift corresponds to the reflection of the field with respect to the z_L axis, i.e., $\mathbf{E}(t, \varphi + 180^\circ) = P_{x_L}\mathbf{E}(t, \varphi)$, and analogously for $\mathbf{A}(t, \varphi)$. Presented results are valid for arbitrary values of the phase φ. The effects of this phase shift for homonuclear diatomic molecules were considered in details in Ref. [29].

When r is even and s is odd the time shift $t \to t + T/2$ [see Eq. (19)], together with the phase shift $\varphi \to \varphi + 180^\circ$, leads to

$$\mathbf{E}(t + T/2, \varphi + 180^\circ) = \mathbf{E}(t, \varphi), \quad r \text{ even}, s \text{ odd}. \tag{22}$$

This means that the phase shift $\varphi \to \varphi + 180^\circ$ leaves the HATI spectrum unchanged in the case of a long laser pulse for any molecule and it's orientation. For combinations of r and s other than in Eq. (22) the phase shift $\varphi \to \varphi + 180^\circ$ generally leads to different spectra transformations.

Let us now analyze the case when r and s are odd for specific orientations $\theta_L = 0^\circ$ and $\theta_L = 90^\circ$. To illustrate the effect of the phase shift $\varphi \to \varphi + 180^\circ$, in Fig. 9, we present the photoelectron momentum distribution for the CO molecule ionized by the ω-3ω OTC laser field with the relative phase $\varphi = 45^\circ$ (left column) and $\varphi = 225^\circ$ (right column). The molecular orientation is $\theta_L = 0^\circ$ (upper panels) and $\theta_L = 90^\circ$ (lower panels). For the molecular orientation $\theta_L = 0^\circ$ the spectra for the relative phases φ and $\varphi + 180^\circ$ are reflected image of each other (reflection is with respect to the k_z axis). As we have mentioned, the phase shift for 180° corresponds to the reflection of the field with respect to the z_L axis. Therefore, for the molecular orientation $\theta_L = 0^\circ$, the 180° phase shift leads to the reflection of the HATI spectrum with respect to the k_z axis. On the other side, for the molecular orientation $\theta_L = 90^\circ$, the HATI spectra obtained for the relative phases φ and $\varphi + 180^\circ$ are reflection images of each other by reflection with respect to the k_x axis. This is the case because the rotation (17) that corresponds to the time shift $t \to t + T/2$ can be presented as two simultaneous reflections, i.e., $R_y(\pi) = P_{x_L}P_{z_L}$. Considered phase shift is equivalent to the action of the operator P_{x_L}, and, since $P_{x_L}P_{x_L} = 1$ and P_{z_L} leaves the molecular orientation $\theta_L = 90^\circ$ virtually unchanged, the corresponding HATI spectra are related through the reflection symmetry with respect to the k_x axis.

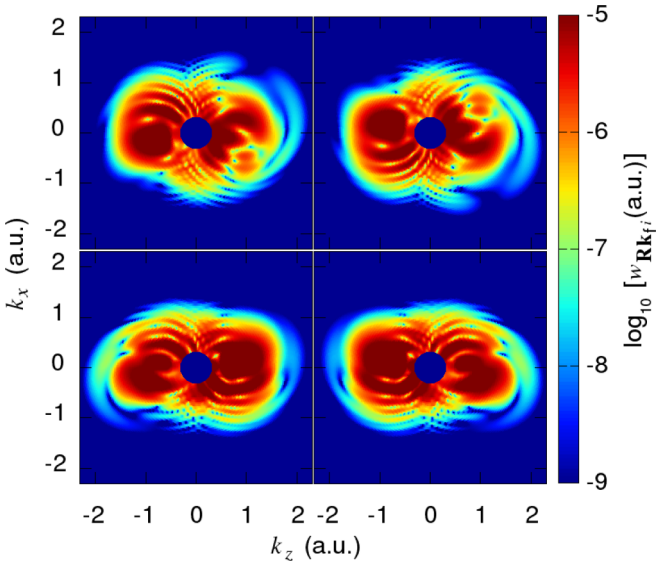

FIG. 9. Logarithm of the differential ionization rate of the CO molecule presented in false colors in the photoelectron momentum plane for the case of ionization by the ω-3ω OTC laser field having the relative phase $\varphi = 45^\circ$ (left) and 225° (right). Molecular orientation angle is $\theta_L = 0^\circ$ for the upper panels, and $\theta_L = 90^\circ$ for the lower panels. The results are obtained using the IMSFA. Other parameters are the same as in Fig. 2.

IV. IMPROVED TWO-DIMENSIONAL SIMPLE MAN'S MODEL WITH IMAGINARY-TIME METHOD

Simple man's model assumes classical motion of the electron in the laser field alone. Solving the Newton equation of motion, $\ddot{\mathbf{r}}(t) = -\mathbf{E}(t)$, we get the velocity

$$\dot{\mathbf{r}}(t) \equiv \mathbf{v}(t) = \mathbf{v}(t_0) + \mathbf{A}(t) - \mathbf{A}(t_0) \tag{23}$$

and the coordinate

$$\mathbf{r}(t) = \mathbf{r}(t_0) + [\mathbf{v}(t_0) - \mathbf{A}(t_0)](t - t_0) + \int_{t_0}^{t} dt' \mathbf{A}(t'). \tag{24}$$

The initial position $\mathbf{r}(t_0)$ depends on whether the ionization happened on the left ($q = 1$) or on the right ($q = -1$) atomic center. To include the rescattering we use the condition that the electron returns to one atomic center at some moment $t = t_1 > t_0$, so that $\mathbf{r}(t_1) = \mathbf{r}(t_0) + (q - q')\mathbf{R}/2$ [$\mathbf{r}(t_1) = \mathbf{r}(t_0)$ if the rescattering happens at the same atomic center ($q' = q$) or $\mathbf{r}(t_1) = \mathbf{r}(t_0) + q\mathbf{R}$ if the rescattering happens at the different atomic center $q' = -q$]. Taking into account Eq. (24), the condition for the electron return becomes

$$(q - q')\mathbf{R}/2 = [\mathbf{v}(t_0) - \mathbf{A}(t_0) - \mathbf{k}_{\rm st}](t_1 - t_0). \tag{25}$$

Since we consider the electrons in the laser-field polarization plane and the molecule is aligned in this plane, Eq. (25) represents a system of two equations which should be solved over the real times t_0 and t_1. For fixed values of the initial velocity $\mathbf{v}(t_0)$ and for fixed q and q', Eq. (25) can have zero, one, or more pairs of solutions (t_0, t_1), depending on the relative phase φ between the laser-field components.

At the time t_1 the electron rescatters off the atomic core (center q') and leaves with the momentum $\mathbf{v}_1$ in the direction θ_1. Using Eq. (23) for the time t_1^- just before the rescattering

($t_1^- = t_1 - \varepsilon$, $\varepsilon \to 0$), we get the electron velocity $\mathbf{v}(t_1^-) = \mathbf{v}(t_0) + \mathbf{A}(t_1^-) - \mathbf{A}(t_0)$. If the direction of the vector $\mathbf{v}(t_1^-)$ in the $z_L x_L$ coordinate system is θ_1^-, then the scattering angle between the vectors $\mathbf{v}(t_1^-)$ and $\mathbf{v}_1$ is $\theta_s = \theta_1 - \theta_1^-$. Taking into account the energy-conservation condition (we assume elastic scattering), we get

$$v_1 = |\mathbf{v}(t_0) + \mathbf{A}(t_1) - \mathbf{A}(t_0)|,$$
$$v_{1z_L} = v_1 \cos\theta_1, \quad v_{1x_L} = v_1 \sin\theta_1. \tag{26}$$

With this new initial electron velocity $\mathbf{v}_1$, the solution of the Newton equation takes the form: $\mathbf{v}(t) = \mathbf{v}_1 + \mathbf{A}(t) - \mathbf{A}(t_1)$ for $t > t_1$. Then the cycle-averaged electron momentum and kinetic energy are ($T = 2\pi/\omega$; see Sec. 5 in Ref. [80])

$$\mathbf{k}_\mathrm{f} = \int_0^T \frac{dt}{T}[\mathbf{v}_1 + \mathbf{A}(t) - \mathbf{A}(t_1)] = \mathbf{v}_1 - \mathbf{A}(t_1),$$
$$E_{\mathbf{k}_\mathrm{f}} = \int_0^T \frac{dt}{2T}[\mathbf{v}_1 + \mathbf{A}(t) - \mathbf{A}(t_1)]^2 - U_p = \frac{\mathbf{k}_\mathrm{f}^2}{2}. \tag{27}$$

To summarize, for fixed q, q', and $\mathbf{v}(t_0)$, we solve Eq. (25) over t_0 and t_1. Then, for different scattering angles θ_s (or, equivalently, the angles θ_1) we calculate $\mathbf{k}_\mathrm{f}$ and $E_{\mathbf{k}_\mathrm{f}}$ using Eqs. (26) and (27). Since the electron emission angle θ_e is determined by the direction of the vector $\mathbf{k}_\mathrm{f}$, for each scattering angle we have obtained a point in the $(\theta_e, E_{\mathbf{k}_\mathrm{f}})$ plane.

Our model can be further improved taking into account that the probability of ionization from one atomic center depends on the initial electron velocity. We can use this probability to adjust the color of the above-mentioned points in the $(\theta_e, E_{\mathbf{k}_\mathrm{f}})$ plane, and thus obtain a false-color presentation which resembles analogous quantum-mechanical presentation of the ionization rate. This ionization probability can be calculated using the formula

$$w_i \propto \exp(-2\,\mathrm{Im}\,W), \tag{28}$$

where W is the so-called shortened action

$$W = \int_{t_\mathrm{in}}^{t_\mathrm{out}} \left[\frac{\mathbf{v}^2(t')}{2} - \mathbf{E}(t')\cdot\mathbf{r}(t') - I_p\right]dt', \tag{29}$$

which can be calculated using the imaginary-time method (see [81] and references therein; for application to the OTC fields see [82,83]). In Eq. (29), $\mathbf{r}(t)$ and $\mathbf{v}(t)$ are the electron position and velocity, respectively, which satisfy the classical Newton equation of motion. The time t_in (t_out) corresponds to the moment when the electron enters (leaves) the tunnel made by the laser field and the atomic potential. The initial conditions for the subbarrier motion are

$$\mathbf{v}^2(t_\mathrm{in})/2 + I_p = 0, \quad \mathbf{r}(t_\mathrm{in}) = \mathbf{0}. \tag{30}$$

The first initial condition assumes that the velocity at the entrance of the tunnel is imaginary, so that the time t_in should be complex. This time should be chosen such that the path is real at the exit of the tunnel, i.e., that $\mathrm{Im}\,\mathbf{r}(t_\mathrm{out}) = \mathrm{Im}\,\mathbf{v}(t_\mathrm{out}) = \mathbf{0}$. According to Eq. (23), the velocity at the exit of the tunnel is

$$\mathbf{v}(t_\mathrm{out}) = \mathbf{v}(t_\mathrm{in}) + \mathbf{A}(t_\mathrm{out}) - \mathbf{A}(t_\mathrm{in}). \tag{31}$$

The time t_out is the ionization time t_0 of our classical simple man's model, so that the velocity at the entrance of the tunnel is

$$\mathbf{v}(t_\mathrm{in}) = \mathbf{v}(t_0) - \mathbf{A}(t_0) + \mathbf{A}(t_\mathrm{in}), \tag{32}$$

and the first equation in Eq. (30) becomes

$$[\mathbf{v}(t_0) - \mathbf{A}(t_0) + \mathbf{A}(t_\mathrm{in})]^2 = -2I_p. \tag{33}$$

For a given initial velocity $\mathbf{v}(t_0)$, Eq. (33) is a nonlinear equation for the complex time t_in. Using solutions of this equation, we can calculate the shortened action W, Eq. (29), and the ionization probability, Eq. (28). It is interesting that Eq. (33) is equivalent to the saddle-point equation for the direct ionization matrix element [1], which has the form $[\mathbf{k}_\mathrm{f} + \mathbf{A}(t_\mathrm{in})]^2 = -2I_p$. This follows from the relation (23), since the cycle-averaged velocity $\mathbf{v}(t)$ is equal to $\mathbf{k}_\mathrm{f} = \mathbf{v}(t_0) - \mathbf{A}(t_0)$. It is known that this saddle-point equation for the $r\omega{-}s\omega$ OTC laser field has $2s$ solutions [84].

To illustrate the usefulness of our improved classical model, in Fig. 10, we compare the photoelectron energy spectra for the CO molecule, calculated using the IMSFA (upper panel) and using the simple man's model with imaginary-time method (lower panel), presented as functions of the emission angle θ_e for the molecular orientation angle $\theta_L = -45^\circ$. The ω-2ω OTC laser field component intensities are equal $E_L^2 = 0.9 \times 10^{14}$ W/cm^2, the fundamental wavelength is 800 nm, and the relative phase is $\varphi = 50^\circ$. For the sake of simplicity, we take into account only the dominant contributions corresponding to the electron ionization from the C center here.

The T-matrix element in the logarithm of the differential ionization rate, which is presented in false colors in the upper panel of Fig. 10, is obtained taking into account only the rescattered electrons which are ionized only from the C center, i.e., $T^{(1)} \approx T^\mathrm{CC} + T^\mathrm{CO}$. For the simple man's model we first choose the initial velocity $\mathbf{v}(t_0)$ such that -1 a.u. $< v_z(t_0) <$ 1 a.u. and -1 a.u. $< v_x(t_0) <$ 1 a.u. For each of these initial velocities, using the algorithm described by Eqs. (25)–(33), we obtain a set of points $(\theta_e, E_{\mathbf{k}_\mathrm{f}})$ with associated probabilities. More precisely, we fix $q = 1$ and obtain two sets of solutions of Eq. (25), one for $q' = 1$ and the other one for $q' = -1$. If we neglect the solutions with the travel time $\tau = t_1 - t_0 > 2T$, for the chosen laser parameters there are four solutions for $q' = 1$, and four solutions for $q' = -1$. If the initial velocity is equal to zero, there are only two solutions for $q' = 1$. One pair of the solutions for $q' = -1$ is similar to the $q' = 1$ solutions: they correspond to the electrons which go away from the center C, turn around, and return and scatter off the center O (center C in the $q' = 1$ case). The second pair of the $q' = -1$ solutions corresponds to the electrons which directly go from the center C and scatter off the center O. For each of these solutions we find the velocity amplitude v_1 and, for the scattering angles $\theta_s \in [0^\circ, 180^\circ]$, we calculate the points in the $(\theta_e, E_{\mathbf{k}_\mathrm{f}})$ plane using Eqs. (26) and (27). The corresponding probabilities are found using the imaginary-time method: for each time t_0 there are $2s = 4$ solutions of Eq. (33) for the complex time t_in. Contribution of one of these solutions is dominant and it is used to calculate the probability w_i using Eqs. (28) and (29). Thus, we have obtained a set of points in the $(\theta_e, E_{\mathbf{k}_\mathrm{f}})$ plane with associated probabilities. These points are plotted in the lower panel of Fig. 10 with false colors corresponding to the calculated probabilities (in arbitrary units and using the logarithmic scale). We see that the

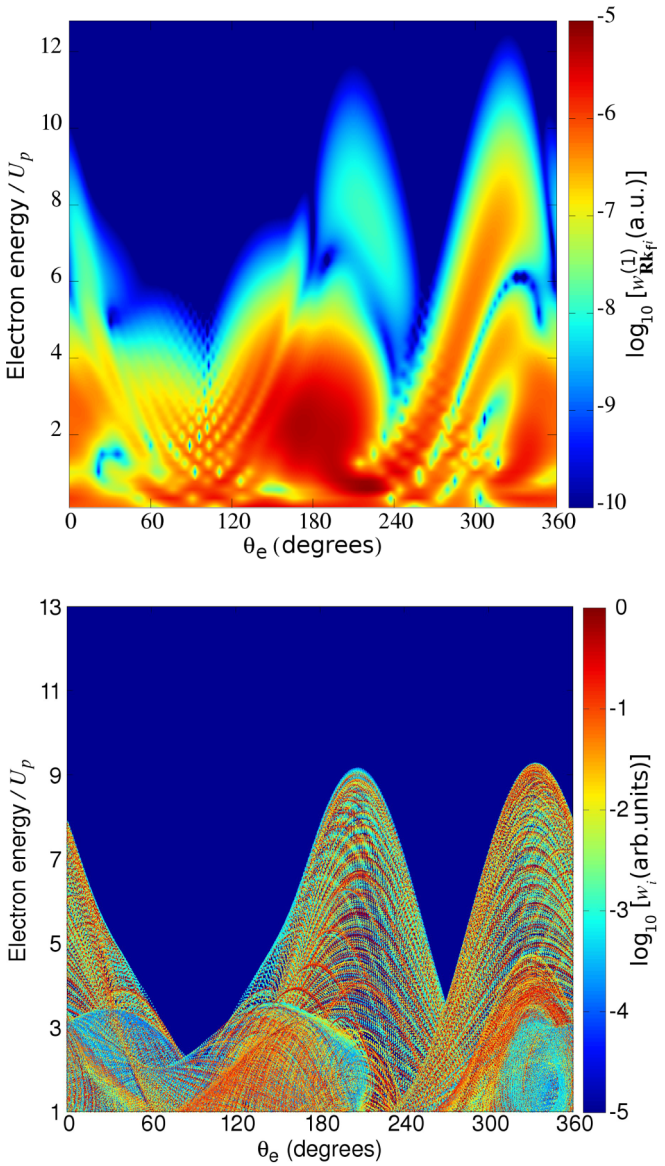

FIG. 10. Upper panel: The logarithm of the photoelectron differential ionization rate, calculated using the IMSFA, for the CO molecule, presented in false colors in the photoelectron emission angle θ_e - photoelectron energy plane. Lower panel: Results analogous to those of the upper panel, but obtained using our two-dimesional simple man's model with the false color scale determined by the ionization probabilities which are obtained using the imaginary-time method. Molecular orientation angle is $\theta_L = -45°$. The molecule is ionized by the ω-2ω OTC laser field having the relative phase $\varphi = 50°$. The laser-field-component intensities are $E_L^2 = 0.9 \times 10^{14}$ W/cm^2 and the fundamental wavelength is 800 nm.

agreement of the quantum-mechanical IMSFA results, presented in the upper panel of Fig. 10, and the results obtained using the semiclassical simple man's model with probabilities calculated using the imaginary-time method, presented in the lower panel of Fig. 10, is excellent. Knowing to which case (different pairs of solutions $q' = 1$ or $q' = -1$) the presented results correspond, we conclude that the low-energy part of the spectrum (with energies lower than $5U_p$) corresponds to the electrons which are ionized at the C center and go directly, having a short travel time, to the O center where they rescatter and leave in the direction of the detector.

V. INTERFERENCE MINIMA CONDITION

The rescattering T-matrix element (16) consists of four contributions (7), which correspond to the situations where the electron is ionized and rescattered at the same or at the different atomic centers. We neglect the Coulomb interaction and consider on an equal footing the scattering off the positive atomic ion and neutral atom which form $(CO)^+$ molecular ion (this approximation may fail for low electron energies). In addition, due to the fact that we are considering heteronuclear diatomic molecules consisting of atoms with not too different nuclear charges (here C, N, and O), we suppose that $V^1_{e\mathbf{K}} \approx V^{-1}_{e\mathbf{K}}$ which is valid for not too different nuclear charges of the constituent atoms. Then, for fixed a and τ, we have

$$\mathcal{F}^{(1)}_{\mathbf{Rk}_f i}(t) \propto \sum_{q,q'} c_{qa} e^{i[q\mathbf{A}(t_0)+q'\mathbf{k}_f+(q-q')\mathbf{k}_{st}]\cdot\mathbf{R}/2}. \tag{34}$$

For heteronuclear diatomic molecules the coefficients c_{1a} and c_{-1a} are not equal up to a sign, as it was the case for homonuclear molecules, but again the interference minima condition can be easily derived. Evaluating the sum over q' Eq. (34) can be written as

$$\mathcal{F}^{(1)}_{\mathbf{Rk}_f i}(t) \propto \cos\left[(\mathbf{k}_f - \mathbf{k}_{st})\cdot\mathbf{R}/2\right] \sum_q c_{qa} e^{iq[\mathbf{k}_{st}+\mathbf{A}(t_0)]\cdot\mathbf{R}/2}. \tag{35}$$

Therefore the destructive interference condition has the following form:

$$R|(k_{f,z} - k_{st,z})\cos\theta_L - (k_{f,x} - k_{st,x})\sin\theta_L| = (2m+1)\pi, \tag{36}$$

where $m = 0, 1, 2, \ldots$.

Let us now analyze the destructive interference minima which appear in the spectra of high-energy electrons. For the parameters used in this paper only the lowest-order ($m = 0$) destructive interference condition can be achieved. For the electrons emitted along the fundamental field component, the components of the final momentum are $k_z = k_f$ and $k_x = 0$, so that the interference minima condition (35) becomes

$$[(k_f - k_{st,z})\cos\theta_L + k_{st,x}\sin\theta_L]^2 = \pi^2/R^2. \tag{37}$$

This nonlinear equation connects the photoelectron energy $E_{\mathbf{k}_f} = \mathbf{k}_f^2/2$ and the molecular orientation angle. The solutions of this equation form a curve in the $(\theta_L, E_{\mathbf{k}_f})$ plane. To determine the stationary momentum we use the quantum-orbit theory and the saddle-point method [1,85]. We solve the system of the saddle-point equations

$$[\mathbf{k}_{st} + \mathbf{A}(t_0)]^2 = -2I_p, \tag{38a}$$

$$[\mathbf{k}_f + \mathbf{A}(t)]^2 = [\mathbf{k}_{st} + \mathbf{A}(t)]^2, \tag{38b}$$

over t_0 and t. The corresponding solutions are complex and can be found in Ref. [84]. For the ω-2ω OTC laser field with the relative phase $\varphi = 180°$ the dominant quantum orbit which is responsible for the high-energy electrons corresponds to $t_0 \approx -0.13T$ and $t \approx 0.48T$. For our purpose we

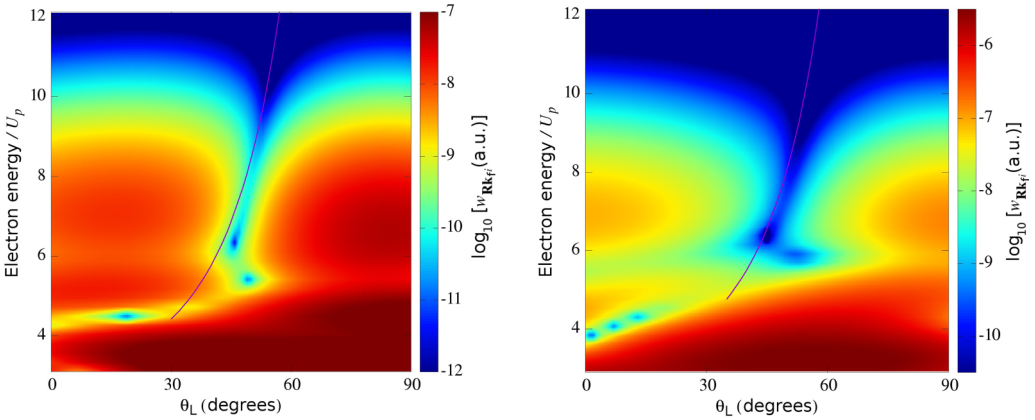

FIG. 11. Logarithm of the differential ionization rate of the CO (left) and NO (right) molecules presented in false colors in the molecular orientation angle -photoelectron energy plane for the case of ionization by the ω-2ω OTC laser field having the fundamental wavelength 800 nm and the intensity of the laser-field components $E_L^2 = 0.9 \times 10^{14}$ W/cm^2. The relative phase is $\varphi = 180^\circ$ and the electrons are emitted in the direction of the fundamental field. The curves which satisfy the destructive interference condition (37) are presented by the violet lines.

have used only the real parts of these solutions to calculate the components of the stationary momentum.

In Fig. 11, we present the logarithm of the differential ionization rate of the CO (left panel) and NO (right panel) molecules in false colors in the $(\theta_L, E_{\mathbf{k}_f})$ plane. The CO and NO molecules are ionized using the ω-2ω OTC laser field and the electrons are emitted in the direction of the fundamental field component, i.e., $\theta_e = 0^\circ$. The intensity of the laser-field components is $E_L^2 = 0.9 \times 10^{14}$ W/cm^2, while the relative phase is $\varphi = 180^\circ$. Using the stationary momentum $\mathbf{k}_{st}$, obtained for the solutions t_0 and t as described above, and Eq. (37) we obtain the curves in the $(\theta_L, E_{\mathbf{k}_f})$ plane. These curves are depicted in Fig. 11 and they nicely follow numerically calculated interference minima. The small deviation from the numerically calculated minima is present due to the contributions of other quantum orbits which are significant in the low- and middle-energy part of the photoelectron spectra. Moreover, in the saddle-point equation (38a) the time-dependent ionization potential $I_p^d(t)$, Eq. (10), is approximated by the constant ionization potential I_p, i.e. the influence of the molecular dipole μ and the polarizabilities $\alpha_\parallel$ and $\alpha_\perp$ is neglected. In principle, it is possible to solve (38) without using this approximation. However, in this case the saddle-point equations have to be solved separately for each molecular orientation angle θ_L. We have checked that for used laser parameters the influence of the molecular dipole $\boldsymbol{\mu}$ and the polarizabilities $\alpha_\parallel$ and $\alpha_\perp$ is small. The main reason for discrepancy of the analytical interference minima curve and the numerical results for low photoelectron energies is the contribution of the other quantum orbits. In addition, the interference minima are present in the HATI spectra regardless of the symmetry of electron-ground-state probability density distribution. In particular, for the CO molecule probability distribution is mostly located on the side of the C atom [37], while for the NO molecule the probability distribution is more homogeneous. However, the interference minima are present in both cases (see Fig. 11). We have also checked that the position of the interference minima does not change significantly as a function of the ratio of the intensities of the laser-field components. Position of the interference minima depends steadily on the wavelength and varies slowly with total field intensity. It also depends on the relative phase. Finally, we note that the larger the difference between nuclear charges of atoms constituting heteronuclear diatomic molecule, the more shallow are the two-center interference minima, and eventually they disappear.

VI. CONCLUSIONS

In this paper, we analyzed high-order above-threshold ionization spectra obtained using the improved molecular strong-field approximation for the case of heteronuclear diatomic molecule aligned in the orthogonally polarized two-color laser-field polarization plane. The OTC-field-component frequencies are $r\omega$ and $s\omega$, with r and s integers.

For $r + s$ odd, we have found a reflection symmetry for the HATI spectra which is valid for arbitrary values of the relative phase φ between the OTC laser field components and component intensity ratio. When r is odd and s is even the HATI spectrum obtained for an arbitrary orientation θ_L is the mirror image of the corresponding HATI spectrum obtained for the molecular orientation $180^\circ - \theta_L$, as given by the relation (20). For r even and s odd, the HATI spectrum, obtained for an arbitrary orientation θ_L, is the mirror image of the corresponding HATI spectrum, obtained for the angle $-\theta_L$, as presented by the relation (21). We have also analyzed the symmetry properties of the HATI spectra for specific molecular orientations $\theta_L = 0^\circ$ and 90°. For $\theta_L = 0^\circ$, when r is even and s is odd, the HATI spectra exhibit reflection symmetry with respect to the k_z axis. When the molecular orientation is $\theta_L = 90^\circ$ and r is odd and s is even, the HATI spectra exhibit reflection symmetry with respect to the k_x axis. This remains valid for arbitrary relative phases φ and component intensity ratio. Comparing this result with the case of homonuclear diatomic molecules it is clear that some reflection symmetries are broken. This is the consequence of the fact that the heteronuclear diatomic molecule is not invariant with respect to the reflection about the axis perpendicular to the internuclear axis. The C_2 rotational symmetry of the HATI spectra for $r + s$ even, which is valid for homonuclear

diatomic molecules [29], is violated for heteronuclear diatomic molecules.

In addition, we have analyzed asymmetries of the photoelectron momentum distributions for heteronuclear diatomic molecules. We have shown that the photoelectron momentum distributions, obtained in ionization by the ω-2ω OTC laser field, are asymmetric for all molecular orientations, except for $\theta_L = 90^\circ$. This holds for arbitrary heteronuclear diatomic molecules and OTC fields with r odd and s even.

Interestingly, partial contributions from an atomic center of the molecule to the total photoelectron spectra can be significant or negligible depending on the electron probability density distribution of the highest occupied molecular orbital but also the molecular orientation. For the CO molecule, the contributions of the case when the electron is ionized from the oxygen atom to the total spectrum are low, while for the NO molecule the differences in contributions of the cases of ionization from the N center and the O center are not so large. We have analyzed the interference of the partial contributions to the T matrix and have shown that total interference result depends on the molecular orientation and on the photoelectron emission angle. We have shown that the maximum photoelectron energy is slightly different for different partial contributions and, therefore, also depends on the molecular orientation and the emission angle.

We have also explored the effect of the phase shift $\varphi \to \varphi + 180^\circ$. This transformation leaves the HATI spectra unchanged if r is even and s is odd. Especially, for the molecular orientation $\theta_L = 0^\circ$ this phase shift leads to the reflection of the HATI spectra with respect to the k_z axis if r is odd and s is even, or if both r and s are odd. Interestingly, for the molecular orientation $\theta_L = 90^\circ$ the phase shift $\varphi \to \varphi + 180^\circ$ leads to the reflection of the HATI spectra with respect to the k_x axis if r and s are both odd.

All above-mentioned symmetries are a consequence of the dynamical symmetry transformations of the OTC laser field and of the reflection symmetries of the heteronuclear diatomic molecule. These symmetries are illustrated using the examples of the HATI spectra for CO and NO molecules and are valid both for the direct and for the rescattered electrons.

We have introduced a two-dimensional simple man's model which assumes classical motion of the photoelectron in the laser field and takes into account different electron initial velocities and electron rescattering at one or the other center of the heteronuclear diatomic molecule. For each of these trajectories, the probability of (direct) ionization is calculated using the imaginary-time method. Having points in the photoelectron emission angle - energy plane and associated probabilities, we presented the photoelectron spectra using false colors in Fig. 10. These results are in excellent agreement with the analogous IMSFA results which are obtained by numerical integration, apart from the intereference effect. Our generalization of the simple man's model provides insights into the dynamics of the ionization process. For example, we know which classical trajectory is responsible for a particular part of the photoelectron spectrum. Knowing this, we are able to control the ionization process.

We have derived and applied a formula for the two-center destructive interference for the case of the ionization of the CO and NO molecules exposed to the ω-2ω OTC laser field. Our analytical formula fits nicely the minima obtained using numerical integration.

Present experimental techniques enable preparation of molecular gases with oriented heteronuclear molecules. For example, impulsive orientation ($\langle\cos\theta\rangle = -0.74$) and alignment ($\langle\cos^2\theta\rangle = 0.82$) of NO molecule was achieved in Ref. [86]. The availability of oriented molecules has opened an avenue of research in strong-field physics, allowing improvements of existing techniques such as tomographic imaging of electronic orbitals [87], multicenter interference effects which reveal molecular structure [88], laser induced-electron diffraction [89,90], fixed-angle broadband laser-driven electron scattering [91,92], time-resolved electron holography [93], etc. We hope that the results presented in our paper will stimulate further development of the mentioned techniques to explore dynamics of photoelectrons ionized from heternuclear diatomic molecules driven by OTC laser fields. If only alignment is achieved in experiment with heteronuclear molecules, symmetries of the corresponding spectra should be as for homonuclear molecules, due to average of contribution of two orientations θ_L and $\theta_L + 180^\circ$.

ACKNOWLEDGMENTS

We gratefully acknowledge support by the Ministry for Education, Science and Youth, Canton Sarajevo, Bosnia and Herzegovina. We also acknowledge support by the Alexander von Humboldt Foundation.

APPENDIX: INVARIANCE WITH RESPECT TO THE REFLECTIONS

We introduce the unitary reflection operator $\mathcal{P}_\mathbf{u}$, which describes the reflection with respect to the plane orthogonal to the unit vector $\mathbf{u}$. Operator of the electron coordinate $\mathbf{r}$ transforms according to [94]

$$\mathbf{r}' = \mathcal{P}_\mathbf{u}\mathbf{r}\mathcal{P}_\mathbf{u}^\dagger = \mathbf{r} - 2\mathbf{u}(\mathbf{u}\cdot\mathbf{r}). \tag{A1}$$

The vectors $\mathbf{k}_\mathrm{f}$ (photoelectron momentum), $\mathbf{R}$ (internuclear coordinate), and $\mathbf{E}(t)$ (electric-field vector) transform under the reflection $P_\mathbf{u}$ as

$$\mathbf{v}' = P_\mathbf{u}\mathbf{v} = \mathbf{v} - 2\mathbf{u}(\mathbf{u}\cdot\mathbf{v}), \quad \mathbf{v} = \mathbf{k}_\mathrm{f}, \mathbf{R}, \mathbf{E}(t). \tag{A2}$$

We suppose that the internuclear coordinate $\mathbf{R}$ is fixed and we consider it as a parameter. Then the total Hamiltonian which describes the dynamics of our system is

$$H(\mathbf{r}, t; \mathbf{R}) = K(\mathbf{r}, \mathbf{R}) + V(\mathbf{r}, \mathbf{R}) + (\mathbf{r} - e_R\mathbf{R})\cdot\mathbf{E}(t), \tag{A3}$$

where $K(\mathbf{r}, \mathbf{R})$ is the kinetic energy operator, the potential $V(\mathbf{r}, \mathbf{R})$ describes the interaction of the atomic centers and the electron in the absence of the laser field, and e_R is the relative charge [19]. Our initial state $|\phi_{\mathbf{R}i}(t')\rangle = |\phi_{\mathbf{R}i}\rangle e^{-iE_it'}$ is represented by the eigenvectors of the time-independent part $K + V$ of the total Hamiltonian (A3), while the final state with the asymptotic momentum $\mathbf{k}_\mathrm{f}$, $|\Phi_{\mathbf{R}\mathbf{k}_\mathrm{f}}(t)\rangle$, corresponds to the total Hamiltonian $H(\mathbf{r}, t; \mathbf{R})$. Then, the ionization amplitude has the form [19]

$$M_{\mathbf{R}\mathbf{k}_\mathrm{f}i}(t, t') = -i\int_{t'}^{t} d\tau \langle\Phi_{\mathbf{R}\mathbf{k}_\mathrm{f}}(\tau)|(\mathbf{r} - e_R\mathbf{R})\cdot\mathbf{E}(\tau)|\phi_{\mathbf{R}i}(\tau)\rangle. \tag{A4}$$

We suppose that the vector $\mathbf{u}$ is orthogonal to the internuclear vector $\mathbf{R}$, i.e., $\mathbf{u}\cdot\mathbf{R}=0$ so that $\mathbf{R}'=\mathbf{R}$, and that the electric field vector satisfies the relation $\mathbf{E}(\tau)=\mathbf{E}'(\tau-T/2)$. Denoting with i' the transformed ground-state vector we have $\mathcal{P}_{\mathbf{u}}|\phi_{\mathbf{R}i}\rangle=|\phi_{\mathbf{R}i'}\rangle$. Using also the relation $\mathcal{P}_{\mathbf{u}}|\Phi_{\mathbf{Rk}_\mathrm{f}}(\tau)\rangle=|\Phi_{\mathbf{Rk}'_\mathrm{f}}(\tau-T/2)\rangle$, we get

$$\begin{aligned}M_{\mathbf{Rk}_\mathrm{f}i}(t,t')&=-i\int_{t'}^{t}d\tau\big\langle\Phi_{\mathbf{Rk}'_\mathrm{f}}(\tau-T/2)\big|\mathcal{P}_{\mathbf{u}}(\mathbf{r}-e_R\mathbf{R}')\cdot\mathbf{E}'(\tau-T/2)\mathcal{P}_{\mathbf{u}}^{\dagger}|\phi_{\mathbf{R}i'}(\tau)\big\rangle\\&=-ie^{iE_iT/2}\int_{t'+\frac{T}{2}}^{t+\frac{T}{2}}d\tau'\big\langle\Phi_{\mathbf{Rk}'_\mathrm{f}}(\tau')\big|(\mathbf{r}'-e_R\mathbf{R}')\cdot\mathbf{E}'(\tau')|\phi_{\mathbf{R}i'}(\tau')\big\rangle=e^{iE_iT/2}M_{\mathbf{Rk}'_\mathrm{f}i'}\left(t+\frac{T}{2},t'+\frac{T}{2}\right).\end{aligned}\tag{A5}$$

Since the ionization amplitude is defined up to a phase factor and we take the limits $t'\to-\infty$ and $t\to\infty$ when we calculate the ionization rate, we have proved that $w_{\mathbf{Rk}_\mathrm{f}i}=w_{\mathbf{Rk}'_\mathrm{f}i'}$, i.e., the differential ionization rate is invariant with respect to the reflection $P_{\mathbf{u}}$ such that $\mathbf{R}'=\mathbf{R}$ and $\mathbf{E}(\tau)=\mathbf{E}'(\tau-T/2)$. The above derivation is generally valid, i.e., not only within the IMSFA. Special cases of this result are Eq. (18) for $\theta_L=90^\circ$, $\mathbf{u}=\mathbf{e}_x=\mathbf{e}_{z_L}$, and Eq. (19) for $\theta_L=0^\circ$, $\mathbf{u}=\mathbf{e}_x=\mathbf{e}_{x_L}$, as we have discussed in Sec. III (see also Fig. 5).

[1] W. Becker, F. Grasbon, R. Kopold, D. B. Milošević, G. G. Paulus, and H. Walther, Above-threshold ionization: From classical features to quantum effects, Adv. At. Mol. Opt. Phys. **48**, 35 (2002).

[2] D. B. Milošević and F. Ehlotzky, Scattering and reaction processes in powerful laser fields, Adv. At. Mol. Opt. Phys. **49**, 373 (2003).

[3] P. Agostini and L. F. DiMauro, The physics of attosecond light pulses, Rep. Prog. Phys. **67**, 813 (2004).

[4] A. Becker and F. H. M. Faisal, Intense-field many-body *S*-matrix theory, J. Phys. B **38**, R1 (2005).

[5] A. Scrinzi, M. Yu. Ivanov, R. Kienberger, and D. M. Villeneuve, Attosecond physics, J. Phys. B **39**, R1 (2006).

[6] M. Lein, Molecular imaging using recolliding electrons, J. Phys. B **40**, R135 (2007).

[7] F. Krausz and M. Ivanov, Attosecond physics, Rev. Mod. Phys. **81**, 163 (2009).

[8] M. Nisoli and G. Sansone, New frontiers in attosecond science, Prog. Quantum Electron. **33**, 17 (2009).

[9] C. Figueira de Morisson Faria and X. Liu, Electron-electron correlation in strong laser fields, J. Mod. Opt. **58**, 1076 (2011).

[10] P. Agostini and L. F. DiMauro, Atomic and molecular ionization dynamics in strong laser fields: From optical to X-rays, Adv. At. Mol. Opt. Phys. **61**, 117 (2012).

[11] W. Becker, X. J. Liu, P. J. Ho, and J. H. Eberly, Theories of photoelectron correlation in laser-driven multiple atomic ionization, Rev. Mod. Phys. **84**, 1011 (2012).

[12] P. B. Corkum, Plasma Perspective on Strong Field Multiphoton Ionization, Phys. Rev. Lett. **71**, 1994 (1993).

[13] K. C. Kulander, K. J. Schafer, and J. L. Krause, in *Super-Intense Laser-Atom Physics*, edited by B. Piraux, A. L'Huillier, and K. Rzaążewski, NATO Advanced Studies Institute, Series B: Physics (Plenum, New York, 1993), Vol. 316, p. 95.

[14] W. Becker, S. P. Goreslavski, G. G. Paulus, and D. B. Milošević, The plateau in above-threshold ionization: The keystone of rescattering physics, J. Phys. B **51**, 162002 (2018).

[15] Y. V. Vanne and A. Saenz, Alignment-dependent ionization of molecular hydrogen in intense laser fields, Phys. Rev. A **82**, 011403(R) (2010).

[16] X. B. Bian and A. D. Bandrauk, Phase control of multichannel molecular high-order harmonic generation by the asymmetric diatomic molecule HeH^{2+} in two-color laser fields, Phys. Rev. A **83**, 023414 (2011).

[17] K. J. Yuan and A. D. Bandrauk, Angle-dependent molecular above-threshold ionization with ultrashort intense linearly and circularly polarized laser pulses, Phys. Rev. A **84**, 013426 (2011).

[18] B. Fetić, and D. B. Milošević, High-order above-threshold ionization of the H_2^+ ion: The role of internuclear distance, Phys. Rev. A **99**, 043426 (2019).

[19] D. B. Milošević, Strong-field approximation for ionization of a diatomic molecule by a strong laser field, Phys. Rev. A **74**, 063404 (2006).

[20] W. Becker, J. Chen, S. G. Chen, and D. B. Milošević, Dressed-state strong-field approximation for laser-induced molecular ionization, Phys. Rev. A **76**, 033403 (2007).

[21] M. Busuladžić and D. B. Milošević, Simulation of the above-threshold-ionization experiment using the molecular strong-field approximation: The choice of gauge, Phys. Rev. A **82**, 015401 (2010).

[22] M. Busuladžić, A. Gazibegović-Busuladžić, D. B. Milošević, and W. Becker, Angle-Resolved High-Order Above-Threshold Ionization of A Molecule: Sensitive Tool for Molecular Characterization, Phys. Rev. Lett. **100**, 203003 (2008).

[23] M. Busuladžić, A. Gazibegović-Busuladžić, D. B. Milošević, and W. Becker, Strong-field approximation for ionization of a diatomic molecule by a strong laser field. II. The role of electron rescattering off the molecular centers, Phys. Rev. A **78**, 033412 (2008).

[24] M. Busuladžić, A. Gazibegović-Busuladžić, and D. B. Milošević, Strong-field approximation for ionization of a diatomic molecule by a strong laser field. III. High-order above-threshold ionization by an elliptically polarized field, Phys. Rev. A **80**, 013420 (2009).

[25] M. Busuladžić, A. Gazibegović-Busuladžić, W. Becker, and D. B. Milošević, Molecular above-threshold ionization with a circularly polarized laser field, Eur. Phys. J. D **67**, 61 (2013).

[26] M. Busuladžić, A. Gazibegović-Busuladžić, and D. B. Milošević, Strong-field ionization of homonuclear diatomic molecules by a bicircular laser field: Rotational and reflection symmetries, Phys. Rev. A **95**, 033411 (2017).

[27] A. Gazibegović-Busuladžić, M. Busuladžić, E. Hasović, W. Becker, and D. B. Milošević, Strong-field ionization of linear molecules by a bicircular laser field: Symmetry considerations, Phys. Rev. A **97**, 043432 (2018).

[28] A. Gazibegović-Busuladžić, M. Busuladžić, A. Čerkić, E. Hasović, W. Becker, and D. B. Milošević, Strong-field ionization of linear molecules by a bichromatic elliptically polarized laser field with coplanar counterrotating or corotating components of different frequencies, J. Phys.: Conf. Ser. **1206**, 012003 (2019).

[29] D. Habibović, A. Gazibegović-Busuladžić, M. Busuladžić, A. Čerkić, and D. B. Milošević, Strong-field ionization of homonuclear diatomic molecules using orthogonally polarized two-color laser fields, Phys. Rev. A **102**, 023111 (2020).

[30] M. Okunishi, R. Itaya, K. Shimada, G. Prümper, K. Ueda, M. Busuladžić, A. Gazibegović-Busuladžić, D. B. Milošević, and W. Becker, Angle-resolved high-order above-threshold ionization spectra for N_2 and O_2: Measurements and the strong-field approximation, J. Phys. B **41**, 201004 (2008).

[31] M. Okunishi, R. Itaya, K. Shimada, G. Prümper, K. Ueda, M. Busuladžić, A. Gazibegović-Busuladžić, D. B. Milošević, and W. Becker, Two-Source Double-Slit Interference in Angle-Resolved High-Energy Above-Threshold Ionization Spectra of Diatoms, Phys. Rev. Lett. **103**, 043001 (2009).

[32] H. Kang, W. Quan, Y. Wang, Z. Lin, M. Wu, H. Liu, X. Liu, B. B. Wang, H. J. Liu, Y. Q. Gu, X. Y. Jia, J. Liu, J. Chen, and Y. Cheng, Structure Effects in Angle-Resolved High-Order Above-Threshold Ionization of Molecules, Phys. Rev. Lett. **104**, 203001 (2010).

[33] A. Gazibegović-Busuladžić, E. Hasović, M. Busuladžić, D. B. Milošević, F. Kelkensberg, W. K. Siu, M. J. J. Vrakking, F. Lépine, G. Sansone, M. Nisoli, I. Znakovskaya, and M. F. Kling, Above-threshold ionization of diatomic molecules by few-cycle laser pulses, Phys. Rev. A **84**, 043426 (2011).

[34] W. Quan, X.-Y. Lai, Y.-J. Chen, C.-L. Wang, Z.-L. Hu, X.-J. Liu, X.-L. Hao, J. Chen, E. Hasović, M. Busuladžić, W. Becker, and D. B. Milošević, Resonancelike enhancement in high-order above-threshold ionization of molecules, Phys. Rev. A **88**, 021401(R) (2013).

[35] W. Quan, X.-Y. Lai, Y.-J. Chen, C.-L. Wang, Z.-L. Hu, X. Liu, X.-L. Hao, J. Chen, E. Hasović, M. Busuladžić, D. B. Milošević, and W. Becker, Quantum orbits: a powerful concept in laser-atom physics, Chin. J. Phys. **52**, 389 (2014).

[36] R. P. Sun, X. Y. Lai, S. G. Yu, Y. L. Wang, S. P. Xu, W. Quan, and X. J. Liu, Tomographic Extraction of the Internuclear Separation Based on Two-Center Interference with Aligned Diatomic Molecules, Phys. Rev. Lett. **122**, 193202 (2019).

[37] E. Hasović, M. Busuladžić, W. Becker, and D. B. Milošević, Dressed-bound-state molecular strong-field approximation: Application to above-threshold ionization of heteronuclear diatomic molecules, Phys. Rev. A **84**, 063418 (2011).

[38] M. Busuladžić, E. Hasović, W. Becker, and D. B. Milošević, Application of the dressed-bound-state molecular strong-field approximation to above-threshold ionization of heteronuclear molecules: NO vs. CO, J. Chem. Phys. **137**, 134307 (2012).

[39] E. Hasović, D. B. Milošević, M. Busuladžić, A. Gazibegović-Busuladžić, and W. Becker, High-order above-threshold ionization of heteronuclear diatomic molecules by a strong laser field with arbitrary polarization, Laser Phys. **22**, 1827 (2012).

[40] K.-J. Yuan, S. Chelkowski, and A. D. Bandrauk, Molecular photoelectron momentum distributions by intense orthogonally polarized attosecond ultraviolet laser pulses, Chem. Phys. Lett. **638**, 173 (2015).

[41] F. Gao, Y. J. Chen, G. G. Xin, J. Liu, and L. B. Fu, Distilling two-center-interference information during tunneling of aligned molecules with orthogonally polarized two-color laser fields, Phys. Rev. A **96**, 063414 (2017).

[42] M.-M. Liu, M. Han, P. Ge, C. He, Q. Gong, and Y. Liu, Strong-field ionization of diatomic molecules in orthogonally polarized two-color fields, Phys. Rev. A **97**, 063416 (2018).

[43] X. Gong, P. He, Q. Song, Q. Ji, H. Pan, J. Ding, F. He, H. Zeng, and J. Wu, Two-Dimensional Directional Proton Emission in Dissociative Ionization of H_2, Phys. Rev. Lett. **113**, 203001 (2014).

[44] Q. Song, P. Lu, X. Gong, Q. Ji, K. Lin, W. Zhang, J. Ma, H. Zeng, and J. Wu, Dissociative double ionization of CO in orthogonal two-color laser fields, Phys. Rev. A **95**, 013406 (2017).

[45] P. V. Demekhin, A. N. Artemyev, A. Kastner, and T. Baumert, Photoelectron Circular Dichroism with Two Overlapping Laser Pulses of Carrier Frequencies ω and 2ω Linearly Polarized in Two Mutually Orthogonal Directions, Phys. Rev. Lett. **121**, 253201 (2018).

[46] J. H. Mun, H. Sakai, and R. González-Férez, Orientation of linear molecules in two-color laser fields with perpendicularly crossed polarizations, Phys. Rev. A **99**, 053424 (2019).

[47] Q. Liao, P. Lu, P. Lan, W. Cao, and Y. Li, Phase dependence of high-order above-threshold ionization in asymmetric molecules, Phys. Rev. A **77**, 013408 (2008).

[48] I. Znakovskaya, P. von den Hoff, S. Zherebtsov, A. Wirth, O. Herrwerth, M. J. J. Vrakking, R. de Vivie-Riedle, and M. F. Kling, Attosecond Control of Electron Dynamics in Carbon Monoxide, Phys. Rev. Lett. **103**, 103002 (2009).

[49] L. Holmegaard, J. L. Hansen, L. Kalhjøj, S. L. Kragh, H. Stapelfeldt, F. Filsinger, J. Küpper, G. Meijer, D. Dimitrovski, M. Abu-samha, C. P. J. Martiny, and L. B. Madsen, Photoelectron angular distributions from strong-field ionization of oriented molecules, Nat. Phys. **6**, 428 (2010).

[50] M. Abu-samha and L. B. Madsen, Effect of multielectron polarization in the strong-field ionization of the oriented CO molecule, Phys. Rev. A **101**, 013433 (2020).

[51] X. Ren and T. Nakajima, Strong-field ionization of a heteronuclear diatomic molecule, Phys. Rev. A **82**, 063410 (2010).

[52] X. Ren and T. Nakajima, Suppression of ionization of heteronuclear diatomic molecules probed by intense lasers, Phys. Rev. A **85**, 023403 (2012).

[53] H. Li, D. Ray, S. De, I. Znakovskaya, W. Cao, G. Laurent, Z. Wang, M. F. Kling, A. T. Le, and C. L. Cocke, Orientation dependence of the ionization of CO and NO in an intense femtosecond two-color laser field, Phys. Rev. A **84**, 043429 (2011).

[54] X. Zhu, Q. Zhang, W. Hong, P. Lu, and Z. Xu, Molecular orbital imaging via above-threshold ionization with circularly polarized pulses, Opt. Express **19**, 13722 (2011).

[55] X. Zhu, Q. Zhang, W. Hong, P. Lu, and Z. Xu, Laser-polarization-dependent photoelectron angular distributions from polar molecules, Opt. Express **19**, 24198 (2011).

[56] X. Liu, Y. Liu, H. Liu, Y. Deng, C. Wu, and Q. Gong, Fully differential measurement on above-threshold ionization of CO and CO_2 molecules in strong laser field, J. Opt. Soc. Am. B **28**, 293 (2011).

[57] B. Zhang, J. Yuan, and Z. Zhao, Dynamic Core Polarization in Strong-Field Ionization of CO Molecules, Phys. Rev. Lett. **111**, 163001 (2013).

[58] X.-B. Bian and A. D. Bandrauk, Orientation-dependent forward-backward photoelectron holography from asymmetric molecules, Phys. Rev. A **89**, 033423 (2014).

[59] T. Endo, A. Matsuda, M. Fushitani, T. Yasuike, O. I. Tolstikhin, T. Morishita, and A. Hishikawa, Imaging Electronic Excitation of NO by Ultrafast Laser Tunneling Ionization, Phys. Rev. Lett. **116**, 163002 (2016).

[60] S. Wang, J. Cai, and Y. Chen, Ionization dynamics of polar molecules in strong elliptical laser fields, Phys. Rev. A **96**, 043413 (2017).

[61] V.-H. Hoang, S.-F. Zhao, V.-H. Le, and A.-T. Le, Influence of permanent dipole and dynamic core-electron polarization on tunneling ionization of polar molecules, Phys. Rev. A **95**, 023407 (2017).

[62] Q. Song, Z. Li, H. Li, P. Lu, X. Gong, Q. Ji, K. Lin, W. Zhang, J. Ma, H. Zeng, F. He, and J. Wu, Orientation-dependent strong-field dissociative single ionization of CO, Opt. Express **25**, 2221 (2017).

[63] Y. Ito, M. Okunishi, T. Morishita, O. I. Tolstikhin, and K. Ueda, Rescattering photoelectron spectroscopy of heterodiatomic molecules with an analytical returning photoelectron wave packet, Phys. Rev. A **97**, 053411 (2018).

[64] C. Zhang, T. Feng, N. Raabe, and H. Rottke, Strong-field ionization of xenon dimers: The effect of two-equivalent-center interference and of driving ionic transitions, Phys. Rev. A **97**, 023417 (2018).

[65] P. Wustelt, F. Oppermann, L. Yue, M. Möller, T. Stöhlker, M. Lein, S. Gräfe, G. G. Paulus, and A. M. Sayler, Heteronuclear Limit of Strong-Field Ionization: Fragmentation of HeH^+ by Intense Ultrashort Laser Pulses, Phys. Rev. Lett. **121**, 073203 (2018).

[66] L. Yue, P. Wustelt, A. M. Sayler, F. Oppermann, M. Lein, G. G. Paulus, and S. Gräfe, Strong-field polarizability-enhanced dissociative ionization, Phys. Rev. A **98**, 043418 (2018).

[67] M. He, Y. Zhou, J. Tan, Y. Li, M. Li, and P. Lu, Imaging charge migration in the asymmetric molecule with the holographic interference in strong-field tunneling ionization, J. Phys. B **51**, 245602 (2018).

[68] T. Endo, H. Fujise, H. Hasegawa, A. Matsuda, M. Fushitani, O. I. Tolstikhin, T. Morishita, and A. Hishikawa, Angle dependence of dissociative tunneling ionization of NO in asymmetric two-color intense laser fields, Phys. Rev. A **100**, 053422 (2019).

[69] W. Hu, Y. Liu, S. Luo, X. Li, J. Yu, X. Li, Z. Sun, K.-J. Yuan, A. D. Bandrauk, and D. Ding, Coherent interference of molecular electronic states in NO by two-color femtosecond laser pulses, Phys. Rev. A **99**, 011402(R) (2019).

[70] Y. Liu, W. Hu, S. Luo, K.-J. Yuan, Z. Sun, A. D. Bandrauk, and D. Ding, Vibrationally resolved above-threshold ionization in NO molecules by intense ultrafast two-color laser pulses: An experimental and theoretical study, Phys. Rev. A **100**, 023404 (2019).

[71] W. Hu, X. Li, H. Zhao, W. Li, Y. Lei, X. Kong, A. Liu, S. Luo, and D. Ding, Sub-optical-cycle electron dynamics of NO molecules: the effect of strong laser field and Coulomb field, J. Phys. B **53**, 084002 (2020).

[72] W. Zhang, P. Lu, J. Ma, H. Li, X. Gong, and J. Wu, Correlated electron-nuclear dynamics of molecules in strong laser fields, J. Phys. B **53**, 162001 (2020).

[73] O. Smirnova, M. Spanner, and M. Ivanov, Coulomb and polarization effects in sub-cycle dynamics of strong-field ionization, J. Phys. B **39**, S307 (2006).

[74] O. Smirnova, M. Spanner, and M. Ivanov, Anatomy of strong field ionization II: to dress or not to dress? J. Mod. Opt. **54**, 1019 (2007).

[75] D. B. Milošević, W. Becker, M. Okunishi, G. Prümper, K. Shimada, and K. Ueda, Strong-field electron spectra of rare-gas atoms in the rescattering regime: enhanced spectral regions and a simulation of the experiment, J. Phys. B **43**, 015401 (2010).

[76] B. A. Zon and E. I. Sholokhov, Quasienergy spectra of a dipolar molecule and of the hydrogen atom, Zh. Eksp. Teor. Fiz. **70**, 887 (1976) [Sov. Phys. JETP **43**, 461 (1976)].

[77] P. W. Atkins and R. S. Friedman, *Molecular Quantum Mechanics*, 3rd ed. (Oxford University Press, Oxford, 2001).

[78] M. W. Schmidt *et al.*, General atomic and molecular electronic structure system, J. Comput. Chem. **14**, 1347 (1993).

[79] M. F. Guest, I. J. Bush, H. J. J. van Dam, P. Sherwood, J. M. H. Thomas, J. H. Van Lenthe, R. W. A. Havenith, and J. Kendrick, The GAMESS-UK electronic structure package: algorithms, developments and applications, Mol. Phys. **103**, 719 (2005).

[80] D. B. Milošević and F. Ehlotzky, Coulomb corrections in above-threshold ionization in a bichromatic laser field, J. Phys. B **31**, 4149 (1998).

[81] V. S. Popov, Imaginary-time method in quantum mechanics and field theory, Phys. At. Nucl. **68**, 686 (2005).

[82] I. A. Kotelnikov, A. V. Borodin, and A. P. Shkurinov, Multiphoton ionization of atoms by a two-color pulse, J. Exp. Theor. Phys. **112**, 946 (2011).

[83] D. S. Bagulov and I. A. Kotelnikov, Theory of multiphoton and tunnel ionization in a bichromatic field, J. Exp. Theor. Phys. **116**, 20 (2013).

[84] A. Jašarević, E. Hasović, R. Kopold, W. Becker, and D. B. Milošević, Application of the saddle-point method to strong-laser-field ionization, J. Phys. A **53**, 125201 (2020); A. Jašarević, Application of the quantum-orbit method to ionization by an orthogonal bichromatic field (in Bosnian), M. Sc. thesis, University of Sarajevo, 2019.

[85] D. B. Milošević, Strong-field approximation and quantum orbits, in *Computational Strong-Field Quantum Dynamics: Intense Light-Matter Interactions*, edited by D. Bauer (De Gruyter Textbook, Berlin, 2016), Chap. VII, pp. 199–221.

[86] O. Ghafur, A. Rouzée, A. Gijsbertsen, W. K. Siu, S. Stolte, and M. J. J. Vrakking, Impulsive orientation and alignment of quantum-state-selected NO molecules, Nat. Phys. **5**, 289 (2009).

[87] J. Itatani, J. Levesque, D. Zeidler, H. Niikura, H. Pépin, J. C. Kieffer, P. B. Corkum, and D. M. Villeneuve, Tomographic imaging of molecular orbitals, Nature (London) **432**, 867 (2004).

[88] T. Kanai, S. Minemoto, and H. Sakai, Quantum interference during high-order harmonic generation from aligned molecules, Nature (London) **435**, 470 (2005).

[89] C. I. Blaga, J. L. Xu, A. D. DiChiara, E. Sistrunk, K. K. Zhang, P. Agostini, T. A. Miller, L. F. DiMauro, and C. D. Lin, Imaging ultrafast molecular dynamics with laser-induced electron diffraction, Nature (London) **483**, 194 (2012).

[90] M. Meckel, D. Comtois, D. Zeidler, A. Staudte, D. Pavičić, H. C. Bandulet, H. Pépin, J. C. Kieffer, R. Dörner, D. M. Villeneuve, and P. B. Corkum, Laser-induced electron tunneling and diffraction, Science **320**, 1478 (2008).

[91] J. Xu, C. I. Blaga, K. Zhang, Y. H. Lai, C. D. Lin, T. A. Miller, P. Agostini, and L. F. DiMauro, Diffraction using laser-driven broadband electron wave packets, Nat. Commun. **5**, 4635 (2014).

[92] M. G. Pullen, B. Wolter, A.-T. Le, M. Baudisch, M. Sclafani, H. Pires, C. D. Schröter, J. Ullrich, R. Moshammer, T. Pfeifer, C. D. Lin, and J. Biegert, Influence of orbital symmetry on diffraction imaging with rescattering electron wave packets, Nat. Commun. **7**, 11922 (2016).

[93] Y. Huismans, A. Rouzée, A. Gijsbertsen, J. H. Jungmann, A. S. Smolkowska, P. S. W. M. Logman, F. Lépine, C. Cauchy, S. Zamith, T. Marchenko, J. M. Bakker, G. Berden, B. Redlich, A. F. G. van der Meer, H. G. Muller, W. Vermin, K. J. Schafer, M. Spanner, M. Yu. Ivanov, O. Smirnova, D. Bauer *et al.* Time-resolved holography with photoelectrons, Science **331**, 61 (2011).

[94] A. Messiah, *Quantum Mechanics* (North-Holland, Amsterdam, 1965).